Master Thesis
TVVR 17/5006

Impacts of the Sea Dike and Reclamation Project in Isahaya Bay on Baroclinic Structure in the Ariake Sea, Japan

Camilla Ranlund

Division of Water Resources Engineering
Department of Building and Environmental Technology
Lund University

Impacts of the Sea Dike and Reclamation Project in Isahaya Bay on Baroclinic Structure in the Ariake Sea, Japan

By:
Camilla Ranlund

Master Thesis

Division of Water Resources Engineering
Department of Building & Environmental Technology
Lund University
Box 118
221 00 Lund, Sweden

Water Resources Engineering
TVVR-17/5006
ISSN 1101-9824

Lund 2017
www.tvrl.lth.se

Master Thesis
Division of Water Resources Engineering
Department of Building & Environmental Technology
Lund University

English title:	Impacts of the Sea Dike and Reclamation Project in Isahaya Bay on Baroclinic Structure in the Ariake Sea, Japan
Author(s):	Camilla Ranlund
Supervisor:	Magnus Larson
Examiner:	Hans Hanson
Language	English
Year:	2017
Keywords:	Stratification; modelling; hypoxia; sea dike; simulation; Ariake Sea;

Acknowledgements

I would like to thank all the people who have helped me during the project and contributed to the results we see today.

First I would like to express my gratitude to Kyushu University and all the people that I have met while in Fukuoka. I would especially like to thank my supervisor Professor Shinichiro Yano for his support, suggestions and guidance throughout the work with this thesis. I would also like to express my gratitude to Assistant Professor Tai and to Mr Kimura, of the Environmental Fluid Dynamics Laboratory, for their help and inputs.

From Lund University I would like to thank my supervisor Professor Magnus Larson at the Department of Water Resources Engineering who has helped me through useful ideas and feedback.

Finally, I am very grateful to all the members of the Environmental Fluid Dynamics Laboratory for their friendship in addition to their continuous support both with my research and in my daily life here in Japan.

Thank you!

Camilla

Abstract

In 1997 the Isahaya Sea Dike was built in the head of Isahaya Bay which is a branch of the Ariake Sea, Japan, with the aim of reclaiming land for agriculture and flood control.

This study examines how the Isahaya Sea Dike has affected the baroclinic structure and development of hypoxic waters in the Ariake Sea by focusing on the spatial change of freshwater discharge, the temporal change of freshwater discharge and the vertical mixing. To accomplish this modelling in Delft3D-FLOW was used to simulate the three scenarios: conditions without the dike (1), conditions with the dike (2) and conditions with the dike but with the Honmyo River discharge from the North Gate (3).

The results show that the spatial change and the temporal change of freshwater due to the construction of the dike has no significant effect on the baroclinic structure in the Ariake Sea. The results also confirms the results by Yano and Nishimura (2014) that the dike has caused weakened vertical mixing in Isahaya Bay. To determine the cause of the development of hypoxic waters in the Ariake Sea further studies are needed.

Sammanfattning

År 1997 byggdes en havsvall i Isahaya bukten i Ariake havet, Japan, för att återta land för lantbruk och översvämningskontroll.

Den här studien undersöker hur havsvallen har påverkat den barokliniska strukturen i Ariake havet och bildandet av hypoxiskt vatten i Ariake havet genom att fokusera på påverkan från förflyttningen av utflödet av färskvatten, den tidsmässiga förändringen för utflödet av färskvatten samt den vertikala omblandningen. För att åstadkomma detta användes modellering i Delft3D-FLOW för att simulera tre scenarier: förhållanden utan havsvallen (1), förhållanden med havsvallen (2) och förhållanden med havsvallen men med utflöde från Honmyo floden från den norra porten (3).

Resultaten visar att den rumsliga förändringen och den tidsmässiga förändringen av färskvatten på grund av byggandet av havsvallen inte har någon signifikant effekt på den barokliniska strukturen i Ariake havet. Resultaten bekräftar också resultaten från Yano och Nishimura (2014) att havsvallen har orsakat försvagad vertikal omblandning i Isahaya bukten. För att fastställa orsaken till utvecklingen av syrefattiga vatten i Ariake havet så behövs ytterligare studier.

Table of contents

1 Introduction

The sea closest to the coast, the shelf sea, occupy only a small part of the total oceans, yet it is of considerable importance to humans and other organisms. About 40% of the human population live close to the sea (Simpson & Sharples, 2012) and are dependent on the resources available. Shelf seas are biologically the oceans' most productive part and support a majority of the world's fisheries. In addition to fish and shellfish the coastal areas are also used extensively for recreation and transport, and are sources of hydrocarbons and renewable energy.

The impacts on the coastal sea by human activity is extensive. The sea is affected by pollution and nutrients coming from the land, by fishing and traffic at sea and by alterations to the coast, such as land reclamation. Land reclamation is when sea area, or coastal wetlands, are removed and the land area is extended to increase agricultural land, make land available for industries or make ports larger. It has been shown that, in some cases, reclamation of land can lead to deterioration of the aquatic environment in the sea. (Simpson & Sharples, 2012)

In 1997 the Isahaya Sea Dike was built in the Ariake Sea, Japan, with the purpose of reclaiming land for agricultural use. After the construction of the sea dike the aquatic environment in the Ariake Sea has deteriorated with smaller fish catches (Nakata, et al., 2010), damage to the cultured laver (Ishizaka, 2003; Ishizaka, et al., 2006), increased algae blooms (Kiyomoto, et al., 2008) and hypoxia in the bottom waters (Tsutsumi, et al., 2003).

There have been a large amount of research conducted to find the reason behind the deteriorating environment in the Ariake Sea though as of yet no principal cause has been found.

1.1 Study area

1.1.1 The Ariake Sea environment

The Ariake Sea, also called the Ariake Bay, is located in the northwestern part of Kyushu Island, Japan, as can be seen in Figure 1. It is a semi enclosed bay surrounded by Fukuoka, Saga, Kumamoto, and Nagasaki prefectures. The tidal range at the head of the Ariake Sea reaches 6m, which is the highest in Japan (Yano, et al., 2009). The sea bay has an average depth of approximately 20m and an area of about 1700km^2 (Yuk, et al., 2011). Through the Hayasaki Straits the Ariake Sea is connected with the East China Sea. The sediment load into the Ariake Sea was estimated to be a mean total of 570 x 10^3 tons per year (Cao Don, et al., 2007). The large tidal flats of about 192km^2 (Yano, et al., 2009) in the Ariake Sea has both areas with sandy bottoms and areas with muddy bottoms (Hiramatsu, et al., 2005). Most of the sea bottom is covered by silt and sand, with generally the sand located offshore and along the shoreline finer-grained sediment (Hiramatsu, et al., 2005).

Together with a large tidal range there is also strong tidal mixing and the amount of freshwater input into the Ariake Sea is large (Nakata, et al., 2010). In Figure 1 all the A-class Rivers and several of the large B-class Rivers discharging into the Ariake Sea are displayed. A-class Rivers are managed by the Japanese government through the Ministry of Land, Infrastructure, Transport and Tourism, while B-class Rivers are managed by the prefectural government. In general the A-class Rivers are large and flows through several prefectures.

The largest river discharging into the Ariake Sea is the Chikugo River located in the inner parts of the Ariake Sea (see Figure 1). The Chikugo River is an A-class river flowing through Fukuoka, Oita and Saga prefectures with a watershed area of 2860 km^2 (Suzuki, et al., 2014; Azhikodan & Yokoyama, 2015) and a length of almost 143 km (Azhikodan & Yokoyama, 2015). In parts due to the inflow from the Chikugo River it is especially into the innermost areas of the Ariake Sea that there is a large input of freshwater. The freshwater from Chikugo River flows counter-clockwise and can, after large amounts of discharge during a short time, leave the head of the Ariake Sea within one week (Yamaguchi & Hayami, 2009).

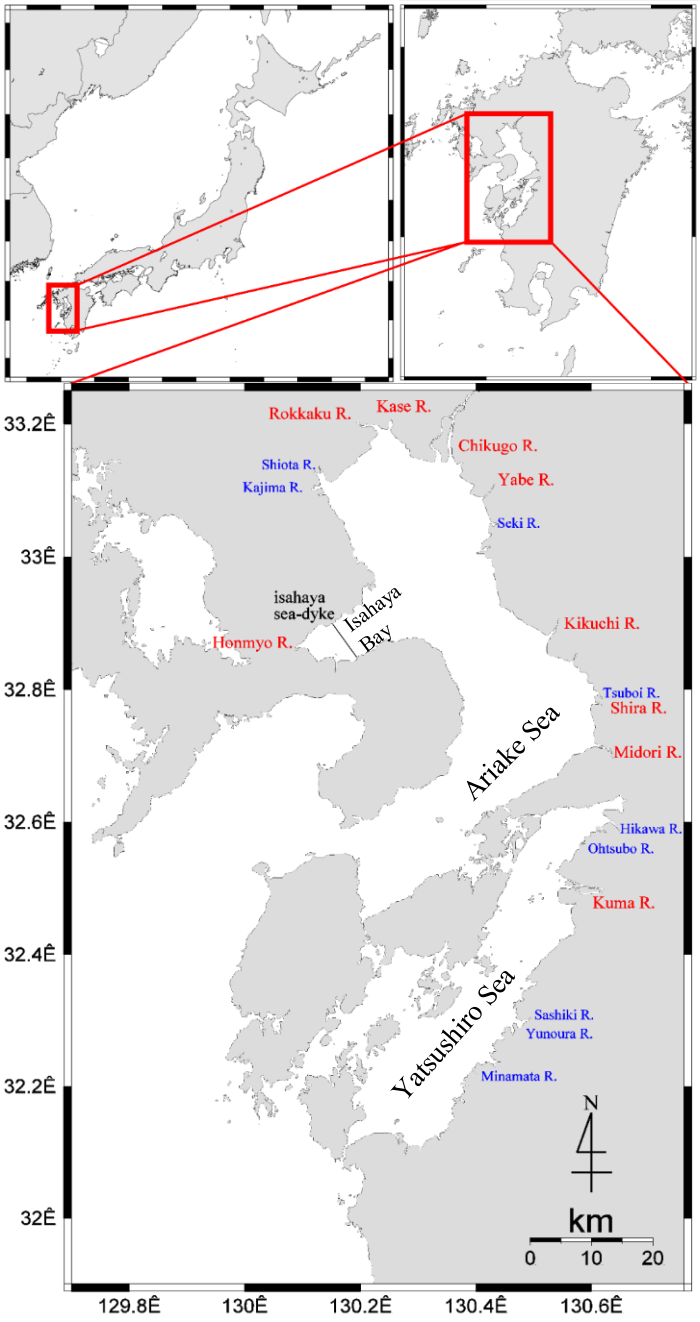

Figure 1 Location of the Ariake Sea including all the A-class Rivers (red) and a number of B-class Rivers (blue) discharging into the Ariake Sea and Yatsushiro Sea.

In Japan there are four different seasons and in the southwest, where the Ariake Sea is located, the climate is subtropical (Japan Meterological Agency a). The precipitation, the daily maximum temperature, the mean temperature and the daily minimum temperature for Fukuoka, located close to the Ariake Sea, can be seen in Figure 2 where the averages of observed data over the consecutive period of 1981-2010 (Japan Meterological Agency c) has been used to create a graph.

During the winter months of December, January and February the Ariake Sea area has moderately cold winters usually with cloudy conditions but with a low amount of precipitation (Japan Meterological Agency b). The spring months of March, April and May consists of gradually rising temperatures, with long sunshine duration at the end of spring (Japan Meterological Agency b). The summer months of June, July and August starts with the rainy season occurring from early June until the middle of July. In Japan northern Kyushu, where the Ariake Sea is located, has one of the highest totals in rainfall. After the rainy season the conditions become very hot, humid and sunny. At times the temperatures can become 35 °C or more (Japan Meterological Agency a). During the autumn months of September, October and November there is a gradual drop in temperature with tropical cyclones and the autumnal rain front affecting the weather together with otherwise sunny conditions (Japan Meterological Agency b). During spring and summer the amount of precipitation is larger than the amount of evaporation in the Ariake Sea whereas during the winter the amount of precipitation is smaller than the amount of evaporation (Yanagi & Abe, 2005).

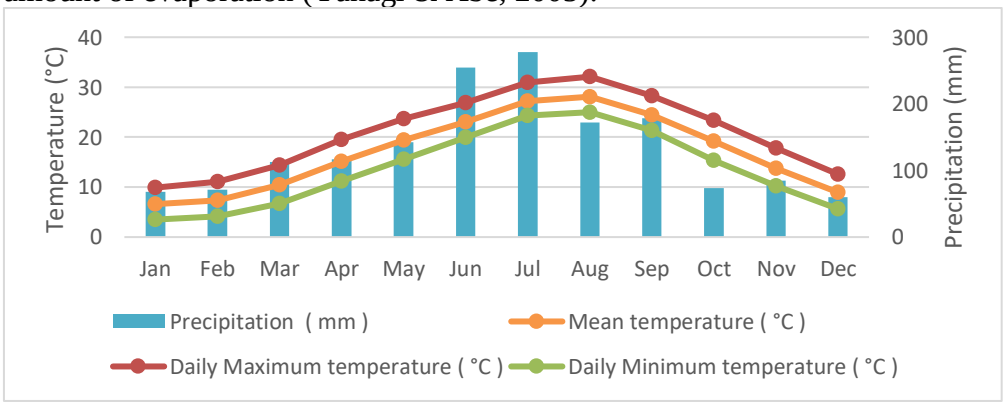

Figure 2 The mean air temperature and precipitation variation in a year with averages of observed data from Fukuoka over the consecutive period of 1981-2010 (Data source: (Japan Meterological Agency c)).

The combined effects of the tidal range, tidal mixing and freshwater could be important in contributing to a multitude of habitats such as a tidal flat and the upholding of a productive environment for fishery resources like shellfish and cultured laver (Nakata, et al., 2010). In Japan the Ariake Sea is one of the most famous seaweed cultivation (cultured laver: Nori in Japanese) areas and there is a large amount of fishing activity in the area thanks to the broad and biologically productive tidal flat. For fisheries the Ariake Sea is one of the most important shallow seas in western Japan (Nakata, et al., 2010).

The topography of the Ariake Sea has been changed by two major projects, the reclamation of land in the inner part of the Sea and the construction of a 7 km long sea-dike (Umehara, et al., 2015) in the head of the Isahaya Bay as seen in Figure 1.

The Isahaya Bay is a sub embayment of the Ariake Sea located at the northwestern side with a surface area of about 65 km^2, excluding the reclaimed land, and a mean depth of about 10 m (Takahashi, et al., 2014). The sea dike was built in 1997 in order to increase the agricultural farming area and act as flood control. From the enclosed area over 6 km^2 has been reclaimed for agricultural purposes (Takahashi, et al., 2014) and a reservoir of 26 km^2 with brackish water, (salinity < 2) has been formed (Umehara, et al., 2015). In total 35 km^2 has been shut off from the rest of the Isahaya Bay and about 15 km^2 of tidal flat has disappeared due to the reclamation project (The Oceanographic Society of Japan, 2005). The 7 km long sea-dike has two gates, the north gate and the south gate, which are both of underflow type (Hayami & Hamada, 2015). The north gate has a width of 200 m and the south gate has a width of 50 m (Hayami & Hamada, 2015). The two gates are opened in order to keep the water in the reservoir at a level of between 1.5 and 1.8 m (Umehara, et al., 2015). Compared to the mean tidal level in the Isahaya Bay outside of the sea-dike the water level in the reservoir is about 1 m lower (Umehara, et al., 2015). The sea dike has resulted in a change in the location of the input of freshwater originating from one A-class river (Honmyo River) into the Ariake Sea (see Figure 1). The freshwater input also changed from being a continuous flow into the bay from the river, with the magnitude depending on the precipitation, to a larger amount of intermittent input of freshwater during a shorter period of time (a few hours around low tide) when the two gates controlling the flow are opened. It should, however be noted that the two gates are not always opened at the same time and for the same amount of time.

According to Yanagi and Abe (2003), and Yanagi and Abe (2005) the Ariake Sea and open ocean water exchange increased between early and late 1990s because the estuarine circulation in the bay had intensified. They also concluded that a decreased tidal amplitude was the cause of the intensification of the estuarine circulation (Yanagi & Abe, 2005). From autumn and spring when there is a small river discharge the estuarine circulation is strong whereas it is weak during summer when there is a large river discharge (Yanagi & Shimomura, 2006).

1.1.2 Previous research

Although the Ariake Sea environment has, as mentioned in the previous section, boasted a high productivity for fishery resources there have been increasing problems with outbreaks of large scale red tides affecting the sea environment. According to Kiyomoto et al. (2008) it is especially in the winter that the number of red tide outbreaks have increased. Large scale diatom red tide outbreaks have been shown to seriously damage the cultured laver in the Ariake Sea (Ishizaka, 2003; Ishizaka, et al., 2006). In addition to the increased outbreak of red tides, hypoxia in the bottom layers of the water has been shown to appear during the summer since 1997 (Tsutsumi, et al., 2003). According to Tsutsumi et al. (2003) both the large scale outbreaks of red tides of diatoms during the autumn and the hypoxic water during the summer has been indicated to appear after heavy rain falls. The occurrence of red-tide could be triggered by the shortage of dissolved oxygen, by increased nutrient release from the bottom sediment, with the consequence of the habitat environment being even more degraded (Nakata, et al., 2010).

It has been shown that since the late 1980s the fish catches have declined continuously but that in the late 1990s the speed of reduction became more pronounced. In particular the species which are very dependent on the bottom habitat environment, and show similarities in their early life, have been prone to a rapid reduction. These species of fish have their spawning sites located in the central bay, for example off Shimabara Peninsula, and then they move to the inner parts of the bay for the larval and juvenile stages. It can therefore be seen a connection between the rapid decline in fish catches and the hypoxia in the bottom waters. (Nakata, et al., 2010)

Due to these increasing environmental problems there have been a large amount of research conducted to find the reason behind the declining environment in the Ariake Sea though as of yet no principal cause has been found. Some of the research has focused on how the building of the Isahaya sea-dike and the reclamation of land has affected the sea environment. Manda and Matsuoka (2006) showed that the Isahaya sea-dike effect on the tidal currents was restricted to the area close to the sea-dike where the tidal currents decreased due to the sea-dike. They also showed that the reclamation in the inner part of the Ariake Sea has caused the tidal currents to decrease by more than 10% in a big area in the inner part of the sea.

Previous research has also shown that stratification in the Ariake Sea is dominated by salinity stratification rather than thermal stratification. The coastal area off the Shimabara Peninsula have a tendency to mix well whereas the coastal area off Ohura and Takezaki tends to stratify. (Yano, et al., 2010 (a))

Yano & Nishimura (2014) compared the situation with and without the Isahaya sea-dike through numerical simulations of tidal current and salinity stratification in case of flood in 2006. They showed that the dike can affect the inner area of the Isahaya Bay and the coastal area off the Shimabara Peninsula through decreasing the velocity of the tidal current and strengthening the salinity stratification. They also showed that the stratification can be strengthened by the dike in spring tide but not in neap tide. In addition to this their results showed that the influences of the dike on the baroclinic structure related to freshwater is dependent on the tide and the flow rate of the rivers.

1.2 Objectives

The purpose of this study was to examine how the construction of the Isahaya Sea Dike has affected the baroclinic structure in the Ariake Sea, Japan. To accomplish this the following questions were addressed

- How has the spatial change of freshwater discharge affected the baroclinic structure in the Ariake Sea? With the construction of the Isahaya Sea Dike the freshwater discharge into the Isahaya Bay and the Ariake Sea was moved from the mouth of the Honmyo River (see Figure 1) to the gates of the sea dike.

- How has the baroclinic structure in the Ariake Sea been affected by the temporal change of freshwater discharge due to the construction of the sea dike? A change from continuous river discharge to intermittent freshwater discharge has occurred due to the construction of the Isahaya Sea Dike. This is due to that freshwater is only discharge from the gates of the sea dike at certain times in order to keep the water level stable inside of the sea dike.

- How has the construction of the Isahaya Sea Dike affected the vertical mixing in the Ariake Sea? What are the differences and similarities between these results and the results of Yano and Nishimura (2014) regarding weakened vertical mixing? Yano and Nishimura (2014) did a similar study called "Numerical analysis on the effect of large reclamation on the baroclinic structure in the Ariake Sea, Japan" where they showed an effect of weakened vertical mixing due to the construction of the sea dike. The difference between the two studies is the freshwater discharge from the Honmyo River (see Figure 1) and the freshwater discharge from the two gates of the Isahaya Sea Dike. In this study these freshwater discharges were taken into account whereas they were not considered in the study by Yano and Nishimura (2014).

- How has the development of hypoxic waters in the Ariake Sea been affected by the construction of the sea dike? Previous research has suggested that one of the reasons behind the recent development of hypoxic waters in the Ariake Sea could be strengthened stratification due to weakened vertical mixing (Unoki & Sasaki, 2007).

2 Physical processes of shallow seas and bays

2.1 Shelf seas

Shelf seas are located in the transition from continent to ocean (Simpson & Sharples, 2012). They are located above the continental shelf, which is an underwater landmass extending from the continents, and consists therefore of relatively shallow water. The continental shelf has a width of 65 kilometers in average (Talley, et al., 2011). The width can vary greatly, ranging from a few kilometres along North and South Americas Pacific coasts to over 1000 kilometres in the Arctic Ocean (Pinet, 2003). The majority of the world's fisheries are located in the shelf seas due to the highly productive waters (Talley, et al., 2011). While the shelf seas make up 9% of the total ocean area and less than 0.5% of the volume they accounts for an approximated 16% of the global production in the oceans (Simpson & Sharples, 2012).

The motion of the shelf sea waters are driven by mechanical forcing by the tides and the atmosphere combined with inputs of buoyancy from heat exchange at the surface and from freshwater (Simpson & Sharples, 2012). The density of seawater is changed by buoyancy forcing (Talley, et al., 2011). For most parts of the shelf the buoyancy input is dominated by the surface heat exchange (Simpson & Sharples, 2012). In Ariake Sea, however, it has been shown that the stratification is dominated by salinity stratification, i.e. the buoyancy input due to freshwater fluxes is dominating (Yano, et al., 2010 (a)). In estuaries and regions of freshwater influence (ROFI) the buoyancy input from heat exchange might be outcompeted by the buoyancy input from freshwater fluxes (Simpson & Sharples, 2012). In the ocean as a whole the mechanical forcing is dominated by surface wind stress (Talley, et al., 2011). In the shelf seas, on the other hand, the mechanical forcing is in many cases dominated by tides instead of by surface wind stress (Simpson & Sharples, 2012).

2.1.1 Tides

Tides are generated from the interaction between the Earth, the Moon and the Sun. The tide generating force, TGF, occurs due to the difference between the gravitational attraction of the Moon, or the Sun, on Earth's centre of mass and the gravitational attraction from the moon, or the Sun, on the ocean (Talley, et al., 2011).

The tides can be broken down into and expressed by tidal constituents (Talley, et al., 2011). These constituents are a result of the characteristics of the orbital movement of the Moon around the Earth and the Earth-Moon system around the Sun (Simpson & Sharples, 2012). The main tidal constituents are shown in table 1.

Table 1 Tidal constituents (Simpson & Sharples, 2012)

Symbol	**Name**	**Period (hours)**
M_2	Principal lunar	12.42
S_2	Principal solar	12.00
N_2	Larger lunar elliptic	12.66
K_2	Luni-solar declination	11.97
K_1	Luni-solar declination	23.93
O_1	Larger lunar declinational	25.82
M_f	Lunar fortnightly	13.7 days

The tide generating force, TGF, at each point on the Earth can be written as a sum of the individual constituents according to

$$TGF = \sum_{n=1}^{N} A_n \cos(\omega_n t + \alpha_n) \quad (1.1)$$

where A_n and α_n are the amplitudes and phases of the constituents. ω_n are frequencies known from the determined motions of the Sun and the Moon (Simpson & Sharples, 2012).

In theory the response to the forcing of the ocean can, if the bathymetry is known, be calculated without using observations. This has however only recently been achieved by using high resolution numerical models (Egbert, et al., 2004). Another way is to consider the observed tide as a sum of harmonic terms with the same frequencies as the TGF but where the phases and amplitudes are different (Simpson & Sharples, 2012) as follows

$$\eta(t) = \sum_{n=1}^{N} H_n \cos(\omega_n t + \alpha_n - g_n) \quad (1.2)$$

where H_n is the amplitudes and g_n is the phase adjustments of the constituents. H_n and g_n can be determined using the least square methods to analyse the observed tidal elevation.

There are about 400 known constituents, i.e. the number of terms N in equations 1.1 and 1.2 is large, but since most of these constituents have small amplitudes the tide can be sufficiently represented by for example about 20 constituents (Simpson & Sharples, 2012). The different tidal components interact to produce spring and neap tides (Talley, et al., 2011). Spring tides are very large tides which occur approximately two times per month when the lunar and solar tides reinforce each other (Talley, et al., 2011). The large spring tides occur when the Moon, the Earth and the Sun are in line and the Moon's high water overlaps with the Sun's high water causing a very high tide to form (Simpson & Sharples, 2012). Neap tides are the smallest high tides which occur between the spring tides, approximately twice a month, when no reinforcement take place (Talley, et al., 2011). The small neap tides occur when the Moon, the Earth and the Sun forms a right angle, i.e. when the Moon's high water overlaps with the Sun's low water which produces a smaller high water (Simpson & Sharples, 2012). For mixing processes the spring-neap cycle can have an important effect.

2.1.2 Regions of Fresh Water Influence

Regions of Freshwater Influence, from here on called ROFIs, are defined as the "region between the shelf sea regime and the estuary where the local input of freshwater buoyancy from the coastal line is comparable with, or exceeds, the seasonal input of buoyancy as heat which occurs all over the shelf" (Simpson, 1997).

In ROFIs the buoyancy input of freshwater produces a physical regime that differs significantly from other areas of the shelf sea (Simpson, 1997). In most parts of the sea the buoyancy of the water is primarily affected by the exchange of heat at the surface (Simpson & Sharples, 2012). This causes the vertical mixing of the waters to be seasonal in most parts of the world. In ROFIs on the other hand the impact of the freshwater causes switching on short time scales between stratified conditions and vertically mixed conditions as a result of the stirring by tides, wave motions and wind stress and because of the changing amount of runoff (Simpson, 1997).

Low salinity water coming from the estuary into the ROFI tends to spread, under the influence of the Coriolis effect, along the coast with the land on its right side (in the Northern Hemisphere). The interaction between the stirring mechanisms and the density driven flow is affected by the topography in the ROFI and how large the forcing is. (Simpson, 1997)

Simpson (1997) described four different types of ROFIs consisting of open coast, corner source, gulf and gulf with sill restriction. These four types depends on shape of the coastline into which the river flows. A gulf type ROFI is a semi enclosed sea with a wide, rounded head and a relatively large river inflow. When it comes to gulf ROFIs, such as the Ariake Sea (Manda & Matsuoka, 2006), there are three main points to understand about the circulation according to Fujiwara et al. (1997). The first point is that it is probable that there will be three different water masses: the river plume, an upper layer with a low salinity concentration and a lower layer with a higher salinity concentration. The second point is that in gulf type ROFIs the rotation by the Earth influences the baroclinic processes at first order. The third point says that a classical longitudal estuarine circulation and the rotation by the Earth are both needed for the resulting circulation to occur.

The freshwater flowing into the ROFI brings contaminants and other land-derived inputs which might cause problems such as eutrophication due to the high input of nutrients. To be able to manage these problems it is important to understand and model the ROFI regime. (Simpson, 1997)

3. Delft3D

For the simulations regarding the Ariake Sea the integrated transport and flow modelling system Delft3D was used, specifically Delft3D-FLOW. The flow in shallow seas, such as the Ariake Sea, coastal areas, estuaries, lagoons, rivers and lakes can be simulated using this flow model (Deltares, 2006). Delft3D was in the study used to simulate three-dimensional (3D) unsteady flow and transport occurrences caused by tidal and meteorological forcing, including density driven flow.

3.1 Approximations and assumptions

Delft3D-FLOW is an advanced model but it is still based on a number of simplifications and assumptions (Deltares, 2006) which is displayed here together with the simplifications used in these simulations.

- The shallow water assumption, the horizontal length is assumed to be much greater than the depth reducing the vertical momentum equation to the hydrostatic pressure relation. This means that vertical accelerations are not taken into accounts since they are assumed to be small compared to the gravitational acceleration.
- Boussinesq approximation, it is only in the pressure term that the effect of variable density is taken into account.
- Reynolds averaging, equations that have been averaged over the length scales of turbulent fluctuations and time are used in Delft3D-FLOW.
- The gravitational acceleration is assumed to be uniform.
- A slip boundary condition is assumed at the bottom.
- In both the vertical and horizontal planes the curvature of the grid is neglected for the horizontal turbulent stresses.
- Through the bed and a closed wall the flux of matter is assumed to be zero.
- If the water depth goes below half of the user defined value the point is set as dry, which means that the velocity becomes zero. When the water depth at the point raises over the limit the point becomes wet again.
- The vertical density differences are considered in the vertical turbulence exchange coefficients and the horizontal pressure gradients but the direct effect on the vertical flow is not taken into account.

- Incompressible water is assumed.
- The water is assumed to be a continuous medium.

3.2 Coordinate system

In Delft3D-FLOW there are several choices for the vertical coordinate system. The σ-coordinate system was originally used in atmospheric models (Phillips, 1957). The purpose of the σ-coordinate system was for the ground to always be a coordinate surface. In Delft3D-FLOW the σ-grid is made up of layers bounded by two sigma planes which follow the free surface and the bottom topography (Deltares, 2006). The two sigma planes are therefore not strictly horizontal and a smooth representation of the topography is obtained. The definition of the σ co-ordinate system is as follows

$$\sigma = \frac{z-\zeta}{d+\zeta} = \frac{z-\zeta}{H} \quad (1.1)$$

where z is the vertical co-ordinate in physical space, ζ is the water level above the reference plane at $z = 0$ (m) and d is the depth below the reference plane (m) (Deltares, 2006). H is the total water depth (m) and is given by

$$H = d + \zeta \quad (1.2)$$

The values of σ is at the free surface $\sigma = 0$ and at the bottom $\sigma = -1$ (Deltares, 2006).

3.3 Basic equations

The numerical hydrodynamic modelling system Delft3D-FLOW solves, in three dimensions, the unsteady shallow water equations. The shallow water equations are derived from the three dimensional Navier-Stokes equations for incompressible free surface flow after averaging over turbulence time-scales. The equations are then called RANS or Reynolds averaged Navier-Stokes equations. To use the shallow water equations the horizontal length scales of flow and bathymetry are assumed to be considerably larger than the depth. Another assumption is that the horizontal accelerations are big compared to the vertical accelerations. This second assumption gives that the vertical momentum equation can be simplified to the hydrostatic pressure relation. (Gerritsen, et al., 2008; Deltares, 2006)

The three-dimensional hydrostatic shallow water equations used in this study are, in the horizontal Cartesian coordinates and in the vertical σ-coordinates, given by (Gerritsen, et al., 2008)

$$\frac{\partial u}{\partial t}+u\frac{\partial u}{\partial x}+v\frac{\partial u}{\partial y}+\frac{\omega}{d+\zeta}\frac{\partial u}{\partial \sigma}-fv=-\frac{1}{\rho}P_u+F_u+\frac{1}{(d+\zeta)^2}\frac{\partial}{\partial \sigma}\left(v_V\frac{\partial u}{d\sigma}\right) \quad (1.3)$$

$$\frac{\partial v}{\partial t}+u\frac{\partial v}{\partial x}+v\frac{\partial v}{\partial y}+\frac{\omega}{d+\zeta}\frac{\partial v}{\partial \sigma}+fu=-\frac{1}{\rho}P_v+F_v+\frac{1}{(d+\zeta)^2}\frac{\partial}{\partial \sigma}\left(v_V\frac{\partial v}{d\sigma}\right) \quad (1.4)$$

$$\frac{\partial \omega}{\partial \sigma}=-\frac{\partial \zeta}{\partial t}-\frac{\partial[(d+\zeta)u]}{\partial x}-\frac{\partial[(d+\zeta)v]}{\partial y}+H(q_{in}-q_{out})+P-E \quad (1.5)$$

In equations 1.3 to 1.5 the horizontal x, y and the vertical σ-directions velocity components are given by u(x,y,σ,t), v(x,y,σ,t) and ω(x,y,σ,t), respectively; t is the time; f is the Coriolis parameter; g is the gravitational acceleration and v_V is the vertical eddy viscosity coefficient. The local sources of water per unit of volume (1/s) is given by q_{in} whereas the local sinks are given by q_{out}. The non-local source term originating from precipitation is given by P and the non-local sink term caused by evaporation is given by E. P_u and P_v are the horizontal pressure terms and are given by equations 1.12 and 1.13. F_u and F_v are the horizontal viscosity terms and are described in equations 1.14 and 1.15. ω in equations 1.3 to 1.5 is calculated from the continuity equation (Gerritsen, et al., 2008) shown below by integrating from the bottom, $\sigma=-1$, to a level σ, $-1\le\sigma\le 0$.

$$\frac{\partial \zeta}{\partial t}+\frac{\partial[(d+\zeta)U]}{\partial x}+\frac{\partial[(d+\zeta)V]}{\partial y}=Q \quad (1.6)$$

where U and V are the depth averaged velocities given by equation 1.7 and 1.8 respectively

$$U=\int_0^{-1}u d\sigma' \quad (1.7)$$

$$V=\int_0^{-1}v d\sigma' \quad (1.8)$$

Q in equation 1.6 above is given by

$$Q=H\int_{-1}^{0}(q_{in}-q_{out})d\sigma+P-E \quad (1.9)$$

3.4 Barotropic and baroclinic effects

The hydrostatic pressure is as follows

$$P = P_{atm} + gH \int_{\sigma}^{0} \rho(x, y, \sigma', t) d\sigma' \quad (1.10)$$

During these simulations constant temperature was assumed giving the following simplified equation for the density

$$\rho = \rho(s) \quad (1.11)$$

where s is the salinity in the range $0.5 < s < 43ppt$.

Leibnitz rule is then used to obtain expressions for the horizontal pressure gradients as described below

$$\frac{1}{\rho} P_u = g \frac{\partial \zeta}{\partial x} + g \frac{d+\zeta}{\rho_0} \int_{\sigma}^{0} \left(\frac{\partial \rho}{\partial x} + \frac{\partial \sigma}{\partial x} \frac{\partial \rho}{\partial \sigma} \right) d\sigma' \quad (1.12)$$

$$\frac{1}{\rho} P_v = g \frac{\partial \zeta}{\partial y} + g \frac{d+\zeta}{\rho_0} \int_{\sigma}^{0} \left(\frac{\partial \rho}{\partial y} + \frac{\partial \sigma}{\partial y} \frac{\partial \rho}{\partial \sigma} \right) d\sigma' \quad (1.13)$$

In the right hand side of the two equations 1.12 and 1.13 the first term describes the barotropic effect and the second term expresses the baroclinic influence. In accordance with the Boussinesq approximation the density variations in equations 1.12 and 1.13 are neglected except in the buoyancy term.

3.5 Horizontal viscosity

With the assumption that the horizontal length is much greater than the water depth (Mellor & Blumberg, 1985) and the flow is a boundary layer flow, the horizontal viscosity terms F_u and F_v in equations 1.3 and 1.4 are given by the following expressions

$$F_u = v_H \left(\frac{\partial^2 u}{\partial x^2} + \frac{\partial^2 u}{\partial y^2} \right) \quad (1.14)$$

$$F_v = v_H \left(\frac{\partial^2 v}{\partial x^2} + \frac{\partial^2 v}{\partial y^2} \right) \quad (1.15)$$

where the horizontal gradients are taken along planes of constant σ-value.

3.6 Coriolis Parameter

The Coriolis parameter *f* is expressed by the following equation

$$f = 2\Omega \sin \phi \quad (1.16)$$

where Ω is the angular speed of rotation of the earth, $\Omega = 7.292 * 10^{-1} s^{-1}$, and ϕ is the geographic latitude.

3.7 Transport equations

In rivers and shelf seas salinity, dissolved substances and/or heat are often transported (Deltares, 2006). In Delft3D-FLOW the transport equations can be used for both the transport of heat and matter. Below is the equation for how the salinity is transported

$$\frac{\partial[(d+\zeta)s]}{\partial t}+\frac{\partial[(d+\zeta)us]}{\partial x}+\frac{\partial[(d+\zeta)vs]}{\partial y}+\frac{\partial(\omega s)}{\partial \sigma}=\left[\frac{\partial}{\partial x}\left(D_h(d+\zeta)\frac{\partial s}{\partial x}\right)+\frac{\partial}{\partial y}\left(D_h(d+\zeta)\frac{\partial s}{\partial y}\right)\right]+\frac{1}{d+\zeta}\frac{\partial}{\partial \sigma}\left[D_v\frac{\partial s}{\partial \sigma}\right]-\lambda_d(d+\zeta)s+S \quad (1.17)$$

where D_h and D_v are the diffusion coefficients in the horizontal and the vertical direction. The λ_d is the first-order decay process. S is the source and sink terms per unit area given by the following equation

$$S=(d+\zeta)(q_{in}s_{in}-q_{out}s)+Q_{tot} \quad (1.18)$$

where s_{in} is the incoming salinity and Q_{tot} is the exchange of heat.

3.8 Turbulence model

In Delft3D-FLOW there are several turbulence models that you can choose from. The turbulence model used was the second order turbulence closure model, k-ε. In the k-ε model the transport equations showed below are used to determine k, the turbulence energy, and ε, the dissipation rate of turbulent kinetic energy.

$$\frac{\partial \mathrm{k}}{\partial \mathrm{t}}+u\frac{\partial k}{\partial x}+v\frac{\partial k}{\partial x}+\frac{\omega}{d+\zeta}\frac{\partial k}{\partial \sigma}=\frac{1}{(d+\zeta)^2}\frac{\partial}{\partial \sigma}\left(D_v\frac{\partial k}{\partial \sigma}\right)+P_k+B_k-\varepsilon \quad (1.21)$$

$$\frac{\partial \varepsilon}{\partial \mathrm{t}}+u\frac{\partial \varepsilon}{\partial x}+v\frac{\partial \varepsilon}{\partial x}+\frac{\omega}{d+\zeta}\frac{\partial \varepsilon}{\partial \sigma}=\frac{1}{(d+\zeta)^2}\frac{\partial}{\partial \sigma}\left(D_v\frac{\partial \varepsilon}{\partial \sigma}\right)+P_\varepsilon+B_\varepsilon-c_{2\varepsilon}\frac{\varepsilon^2}{k} \quad (1.22)$$

where P_k is the production term in transport equation for turbulent kinetic energy, P_ε is the production term in transport equation for the dissipation of turbulent kinetic energy, P_k is the buoyancy flux term in transport equation for turbulent kinetic energy, B_ε is the buoyancy flux term in transport equation for the dissipation of kinetic energy and $c_{2\varepsilon}$ is a calibration constant at a value of 1.92.

Using k and ε the mixing length L is calculated which means that the mixing length becomes a property of the flow. In turn this leads to that no damping functions are needed if stratification occurs. The viscosity can also be determined from k and ε.

4 Calibration and validation

The model used in these simulations has been used in simulations before. Yano et al. (2009) conducted calibration and validation on the numerical model taking into account that the Isahaya Sea dike is closed. After trial and error for the tuning coupled with statistical analysis they achieved highly accurate simulation. In addition to the Chezy friction coefficient of $C=50m^{1/2}/s$ the best combination of parameters found by Yano et al. (2009) is shown in Table 2.

Table 2 Harmonic Constant of Four Major Tides for Open Boundary Condition (Yano, et al., 2009)

		Akune Station	Kabashima Station
M_2	Amplitude (cm)	71.7	86
	Phase (deg.)	211	219
S_2	Amplitude (cm)	31.4	36
	Phase (deg.)	229	240
K_1	Amplitude (cm)	22.9	25
	Phase (deg.)	209	205
O_1	Amplitude (cm)	17.7	19
	Phase (deg.)	185	186

Nishimura et al. (2013) also performed a study of validation with the same model. Their validation was first conducted on how well the simulations express the movement of the freshwater flowing into the Ariake Sea from the Chikugo River. Then they evaluated how well the simulations express the salinity at different depth at one point in the Ariake Sea. The evaluation regarding the movement of the freshwater from the Chikugo River was conducted using the data from field observations performed by Saita et al. (2008). Saida et al. (2008) released a bouy at the river mouth of the Chikugo River and then recorded the movement of the bouy at two different occasions. Observation 1 was on the 7th of June 2006 when the river discharge from the Chikugo River was very low. Observation 2 was on the 21st of July 2006 when the river discharge from the Chikugo River was 4000 m^3/s. The results from these field observations can be seen in Figure 3 below.

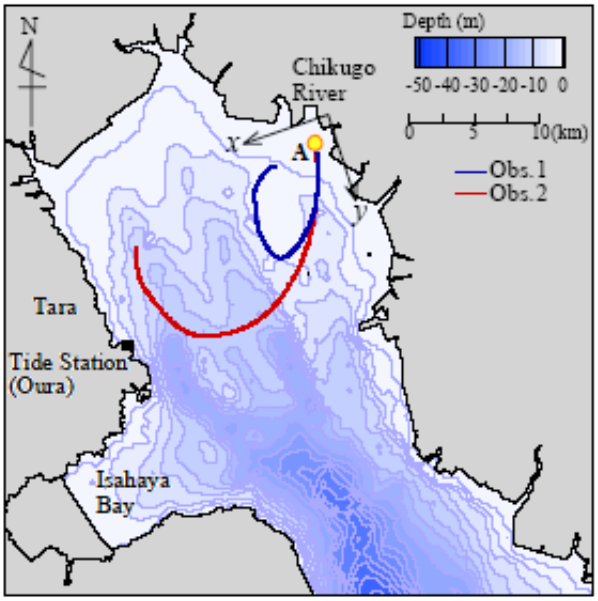

Figure 3 Trajectory of a drifting buoy (Saita, et al., 2008)

Nishimura et al. (2013) then simulated the movement of a buoy to compare with the trajectory recorded by Saita et al. (2008). The results from these simulations can be seen in Figure 4 for observation 1 and in Figure 5 for observation 2. As can be seen from these figures Nishimura et al (2013) also simulated the trajectory of the buoy if it would have been released at different locations close to the river mouth of the Chikugo River.

During the observations by Saita et al. (2008) the buoy might have been affected by wind since it was floating. To account for this possibility Nishimura et al. (2013) added the influence of wind but they could not see any significant difference between applying the wind and not applying the wind.

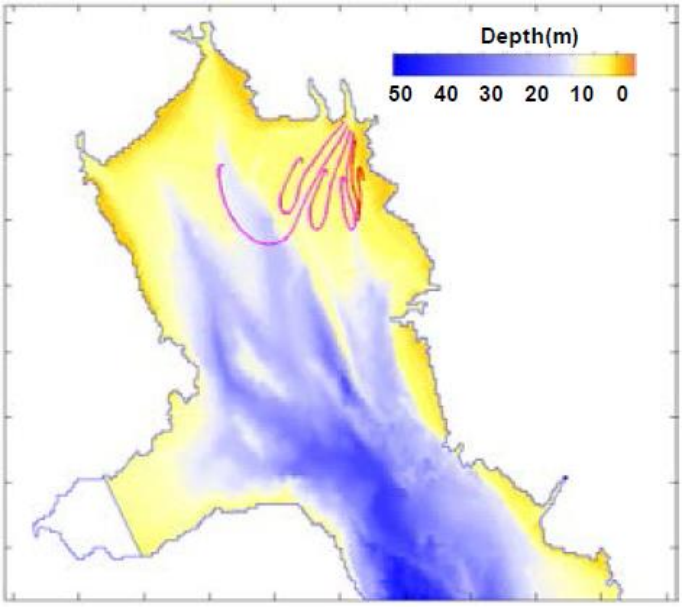

Figure 4 Trajectory of the buoy according to simulations for the 7th of June 2006 (Nishimura, et al., 2013)

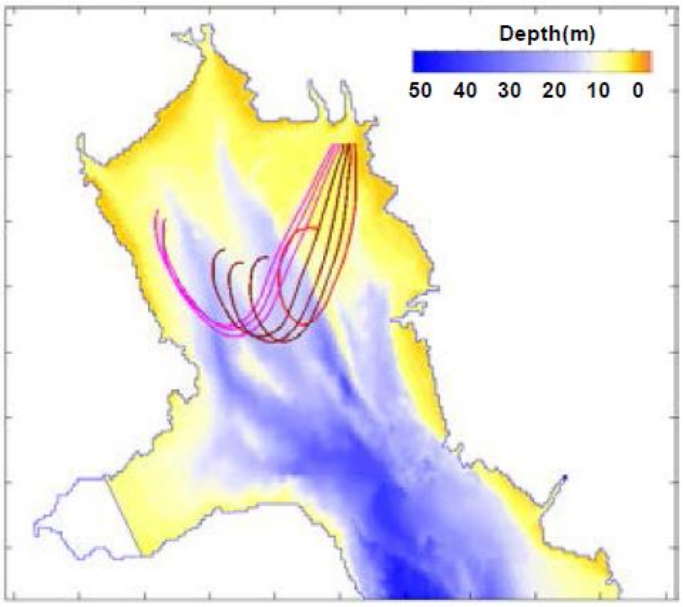

Figure 5 Trajectory of the buoy according to simulations for the 21st of July 2006 (Nishimura, et al., 2013)

From the simulations Nishimura et al. (2013) could show that the behaviour of the buoy is dependent on where it is released. They also concluded that this evaluation shows that the model is accurate to an adequate level to reproduce how the freshwater flows in the Ariake Sea in the area close to the Chikugo River.

The evaluation regarding how well the simulations can express the salinity at different depth in the Ariake Sea was conducted at point B4 located close to the Isahaya Sea-dike as shown in Figure 6. In point B4 Nishimura et al. (2013) obtained continuous data regarding the salinity.

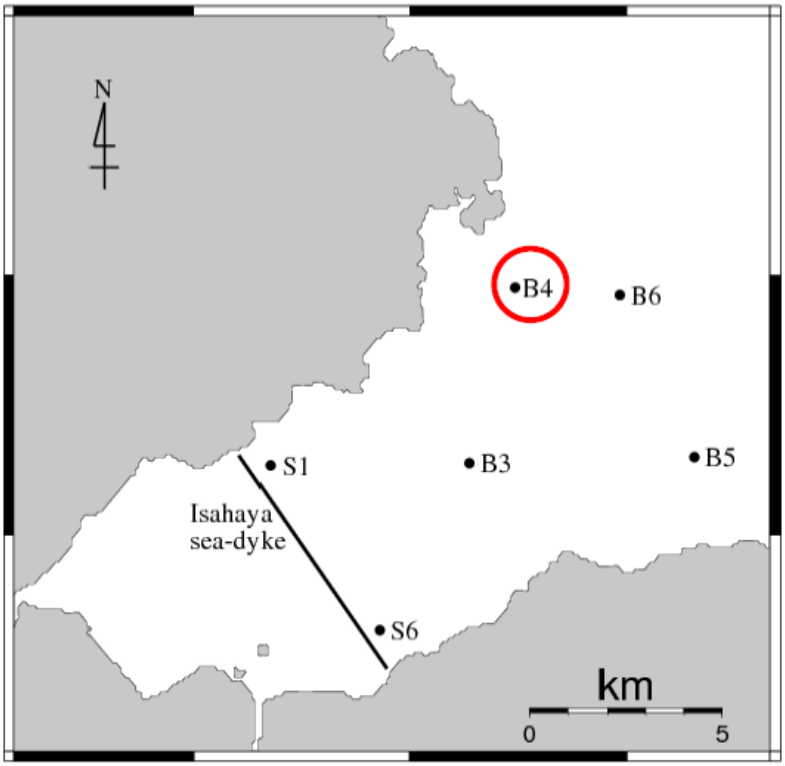

Figure 6 The location of the observation point B4 inside the Isahaya Bay (Nishimura, et al., 2013)

The time for their comparison between the simulations and the observed salinity distribution was from the 19th of July 2006 until the 29th of July 2006. Nishimura et al. (2013) conducted two simulations, one simulation where the wind was taken into consideration and one simulation where the wind was not taken into account. The wind conditions between the 19th of July 2006 and the 29th of July 2006 are shown in Figure 7. For the simulation where the wind was taken into account the resulting salinity distribution can be seen in Figure 8. For the simulation where the wind was not taken into account the resulting salinity distribution can be seen in Figure 9. Nishimura et al. (2013) then compared these two salinity distributions with the observed salinity distribution shown in Figure 10.

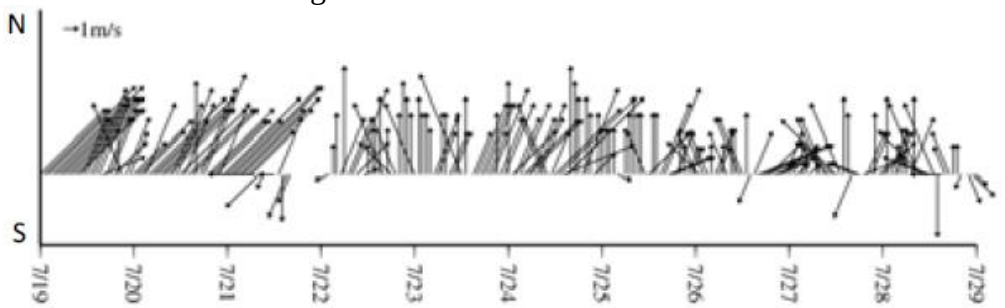

Figure 7 The wind conditions (Nishimura, et al., 2013)

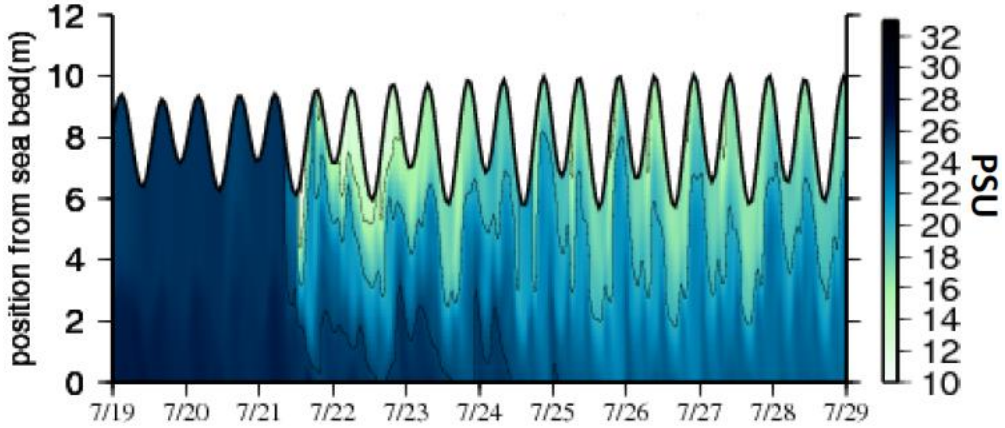

Figure 8 The simulation results for the salinity distribution with wind taken into account (Nishimura, et al., 2013)

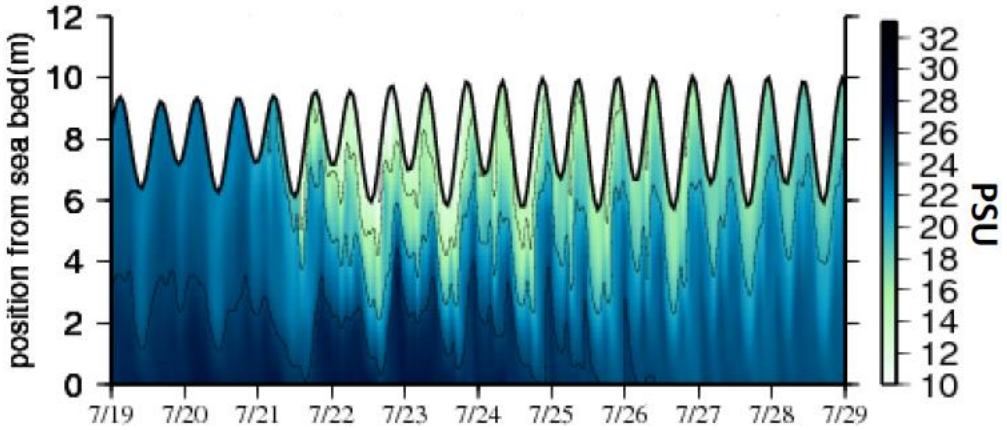

Figure 9 The simulation results for the salinity distribution without wind taken into account (Nishimura, et al., 2013)

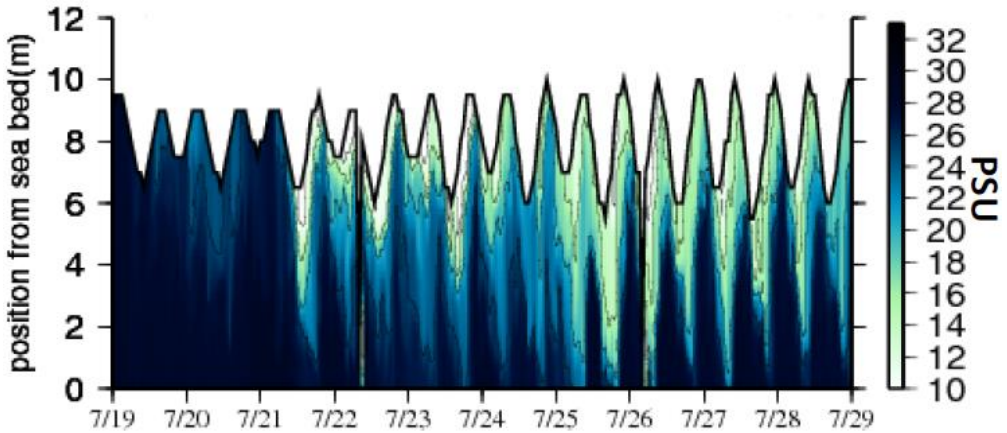

Figure 10 The observation results for the salinity distribution (Nishimura, et al., 2013)

As can be seen in Figures 8-10 the result with the wind, Figure 8, is not more accurate than without the wind, Figure 9. According to Nishimura et al. (2013) the reason behind this might be that the same data for the wind speed and wind direction, Figure 7, was used for all of the Ariake Sea. This data was from the Shimabara observation station which is not located that close to the observation point B4.

Nishimura et al. (2013) suggested two possible reasons why the salinity distribution from the simulations differ from the observed salinity distribution. According to them one reason could be that they put the salinity as constant for the open boundary. Another possible reason that they mention is that the starting value used for the salinity could have been slightly wrong. To improve the accuracy for the simulations more precise physical parameters could be included.

5 Model simulation for different scenarios

The numerical model used in this study was developed by Yano et al. (2010 (b)) by applying Delft3D-FLOW (Deltares, 2006). The computational range, shown in Figure 11, combines the Ariake Sea and the Yatsushiro Sea. The horizontal grid applied in the model was a rectangular grid, Cartesian frame of reference, which in Delft3D-FLOW is considered as a simplified version of a curvilinear grid (Deltares, 2006). For the vertical grid the σ-coordinate system, originally used in atmospheric models (Phillips, 1957), was applied in the model. The number of vertical layers used in these simulations were 10 where, counting from the surface, the three top layers consisted of 5% of the total depth each, the four following layers consisted of 10% of the total depth each and the three bottom layers consisted of 15% of the total depth each (Figure 12). As can be seen the relative layer thickness is non-uniform, which was done in order to obtain more accurate results closer to the surface. The number of vertical layers is independent of the local water depth and constant over the horizontal computational area (Deltares, 2006).

An open boundary was set as a line connecting Akune to Kabashima, shown in Figure 11. For the open boundary conditions 40 tidal components were inputted. These 40 tidal components were based on the known harmonic constants at Akune and Kabashima. For the four major tidal components M2, S2, K1 and O1 the harmonic constants, amplitude and lag, were adjusted to the measurement results at several tide gauges (Yano, et al., 2010 (b)). Figure 13-15 shows the tidal curves for June, July and August 2006 respectively.

Hourly discharge from eight A-class rivers (Ministry of Agriculture, Forestry and Fisheries of Japan, 2008) and nine B-class rivers were used in all of the simulations with the model. The eight A-class rivers were Chikugo River, Yabe River, Kase River, Rokkaku River, Kikuchi River, Shira River, Midori River and Kuma River (Ministry of Land, Infrastructure, Transport and Tourism of Japan, 2015). The nine B-class rivers were Shiota River, Kajima River, Seki River, Tsuboi River, Hikawa River, Ohtsubo River, Sashiki River, Yunoura River and Minamata River. Table 3 shows the catchment areas and discharge information for the eight A-class rivers. Table 4 shows the catchment areas and discharge information for the nine B-class rivers.

The discharge (m^3/s) for the A-class rivers, Q_A, were calculated as follows

$$Q_A = Q_{measure} * \frac{A_{A,tot}}{A_{A,upper}} \quad (1.23)$$

where $Q_{measure}$ is the discharge at the measurement point in m^3/s, $A_{A,tot}$ is the total catchment area m^3 and $A_{A,upper}$ is the catchment area above the measurement point in m^3.

The discharge (m^3/s) for the B-class rivers, Q_B, were calculated according to the following equation

$$Q_B = Q_{A,closest} * \frac{A_B}{A_{A,closest,tot}} \quad (1.24)$$

where $Q_{A,closest}$ is the discharge in m^3/s for the closest A-class river, A_B is the catchment area of the B-class river in m^3 and $A_{A,closest,tot}$ is the catchment area of the A-class river in m^3 for the closest A class river.

Table 3 Catchment area, discharge and station information for A-class rivers

Name A-class river	**Yearly mean discharge (m^3/s)**	**Total catchment area (km^2)**	**Catchment area at discharge station (km^2)**	**Factor**	**Max. discharge (m^3/s)**
Chikugo	95.09	2863	2295	1.25	3119
Yabe	21.54	647	460	1.41	2752
Kase	14.1	368	231	1.59	1039
Rokkaku	4.36	341	95	3.59	1094
Honmyo	2.11	87	35.8	2.43	721
Kikuchi	39.56	996	906	1.10	4274
Shira	25.39	480	477	1.01	1761
Midori	36.17	1100	681	1.62	2686
Kuma	119.92	1880	1868	1.01	6953

Table 4 Catchment area, discharge and information used in the calculations for B-class rivers

Name B-class river	**Yearly mean discharge (m^3/s)**	**Total catchment area (km^2)**	**A-class river for estimation**	**Estimated max. discharge (m^3/s)**
Shiota	0.77	60.4	Rokkaku	194
Kajima	1.61	125.7	Rokkaku	403
Seki	1.59	47.8	Yabe	203
Tsuboi	7.50	141.7	Shira	520
Hikawa	9.48	148.6	Kuma	550
Outsubo	2.21	34.6	Kuma	128
Sasiki	4.27	67	Kuma	248
Yunoura	2.71	42.5	Kuma	157
Minamata	8.45	132.5	Kuma	490

The hydrographs for June, July and August respectively, for the seven A-class rivers discharging into the Ariake Sea, are shown in Figure 13-15. The numerical simulations were conducted for a period of 1 year from the 1st of January 2006 until the 1st of January 2007. For the results the months of June, July and August were then used. During these simulations the second order turbulence closure model, k-ε, was used. The wind was neglected during the simulations and assumed to be zero in accordance with the validation results of Nishimura et al. (2013). The temperature was assumed to be constant to only focus on the salinity stratification since previous research has shown that salinity stratification dominates in the Ariake Sea (Yano, et al., 2010 (a)). For Japan the geographic latitude is $\phi = 0.7 \sim 1.0 * 10^{-4} s^{-1}$ so this was used in the numerical simulations. The initial conditions were set as uniform values at 34 ppt for the salinity and 0 m for the water level.

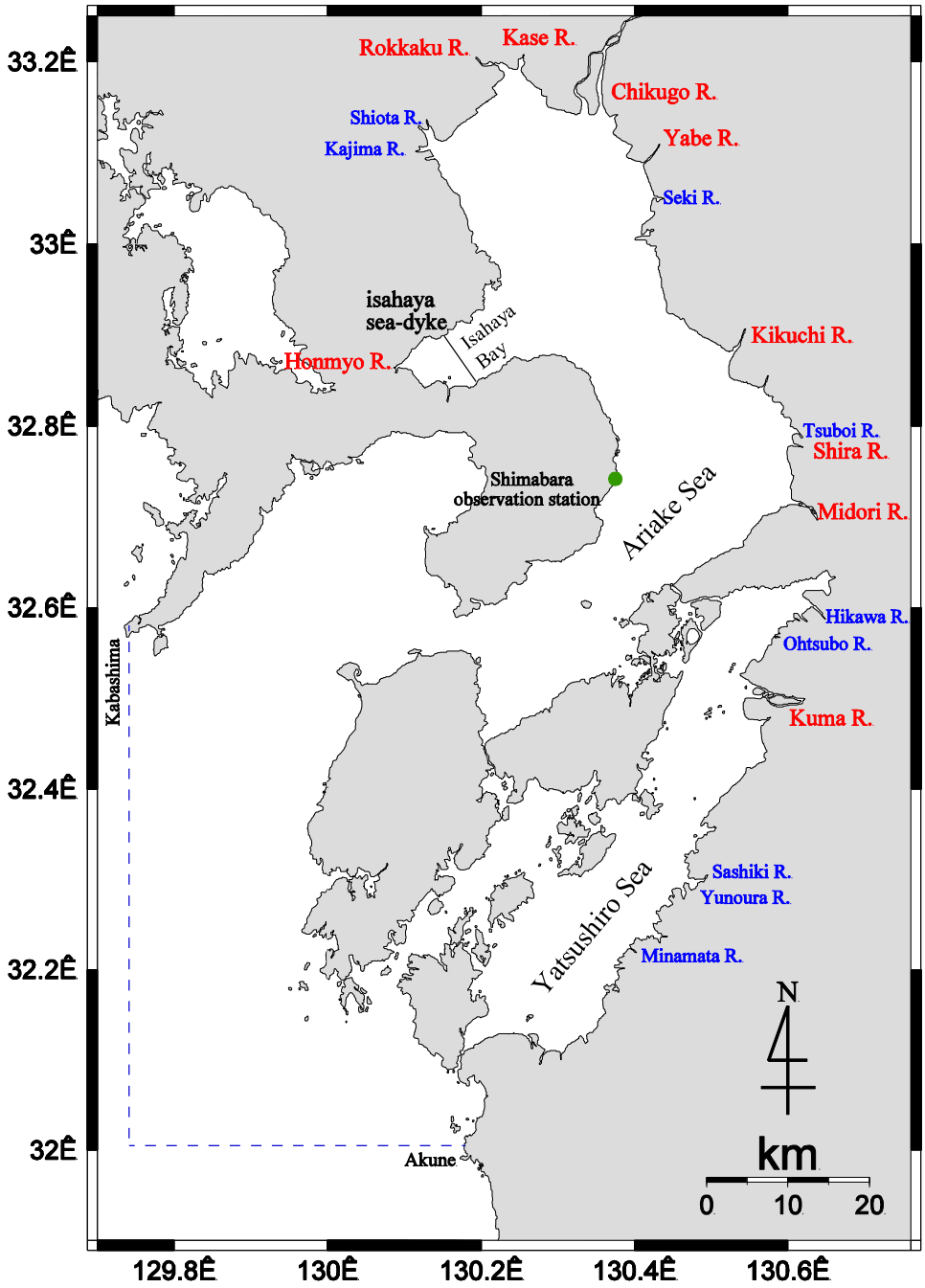

Figure 11 Computational domain

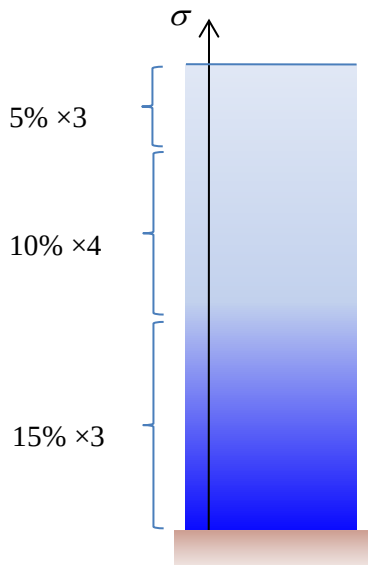

Figure 12 Vertical layers used in the simulations

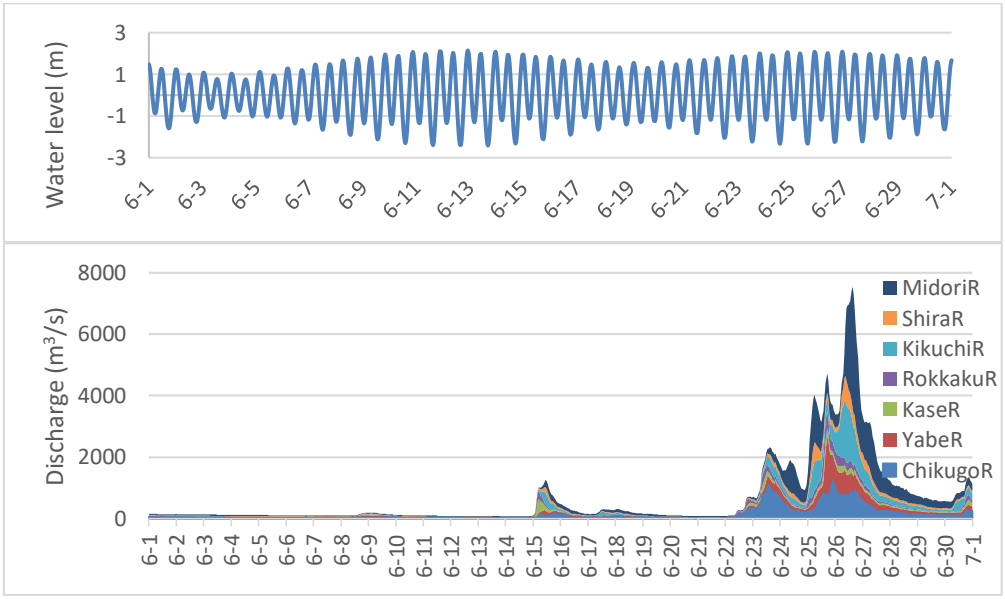

Figure 13 Tidal curve (above) and hydrograph (below) for June 2006 for seven A-class Rivers

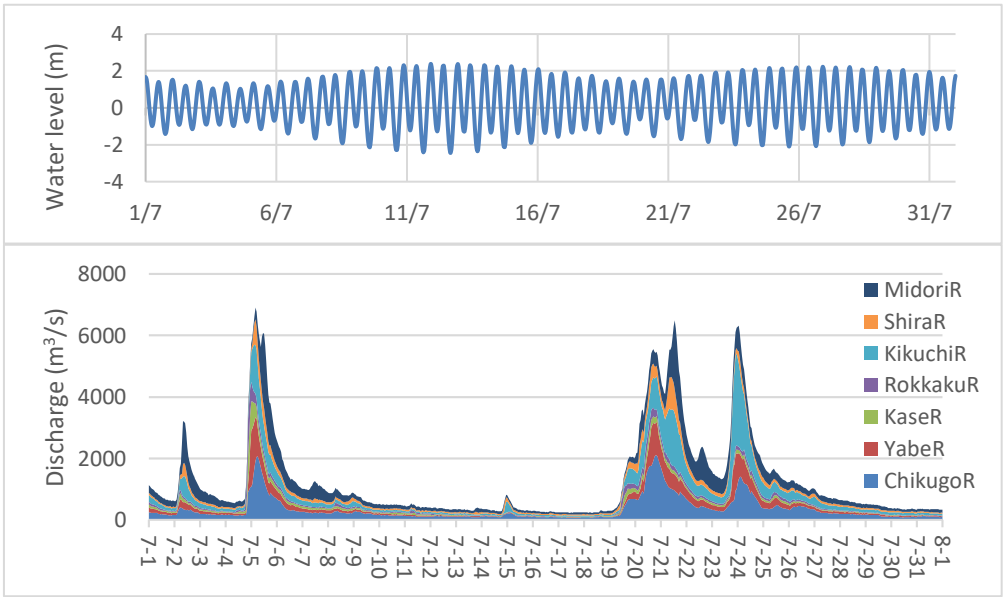

Figure 14 Tidal curve (above) and hydrograph (below) for July 2006 for seven A-class Rivers

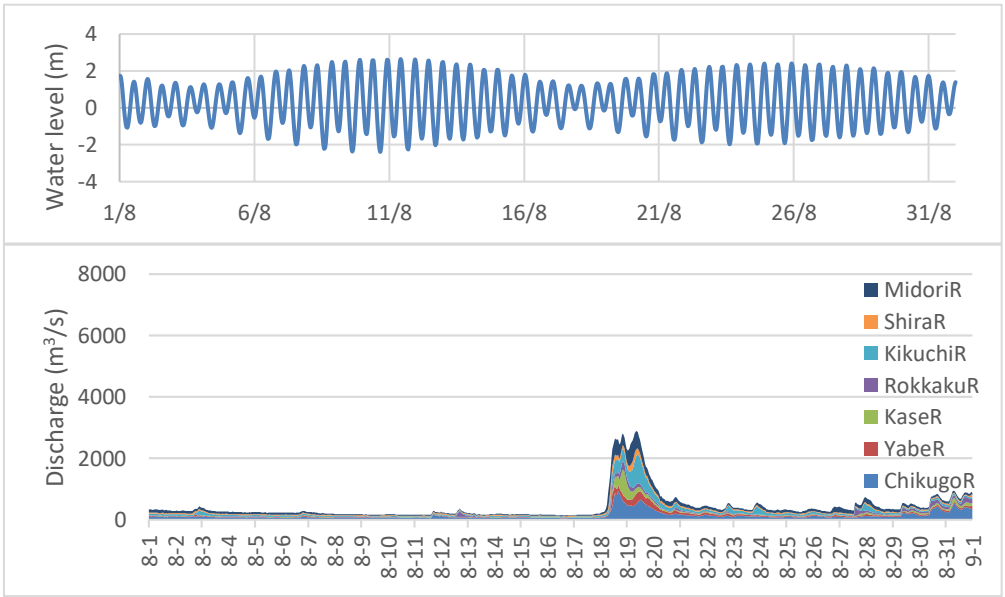

Figure 15 Tidal curve (above) and hydrograph (below) for August 2006 for seven A-class Rivers

5.1 Scenario (1): Conditions without dike

This scenario was conducted in order to reproduce the conditions that existed in the Ariake Sea before the Isahaya Sea dike was built and to see how the baroclinic structure in the Ariake Sea would have been if these conditions were present during 2006. The computational domain used was therefore like Figure 11 without the Isahaya Sea dike. In this scenario hourly discharge from the A-class River called Honmyo River (Ministry of Land, Infrastructure, Transport and Tourism of Japan, 2015) was used in addition to the discharge data used in all of the scenarios. The discharge was calculated according to equation 1.23. Table 3 shows the catchment area, discharge and station information for Honmyo River.

The total water volume (m^3) that came from the Honmyo River into the Ariake Sea during 2006, $V_{tot,H}$, was calculated according to

$$V_{tot,H} = \sum Q_H * t_H \quad (1.25)$$

where Q_H is the discharge from the Honmyo River at each time step in m^3/s and t_H is a constant time at 3600 seconds.

Using Equation 1.25 the total water volume from the Honmyo River during 2006 was calculated to $1.09 * 10^8 m^3$. Figure 16 shows the hydrographs for the Honmyo River during June, July and August 2006.

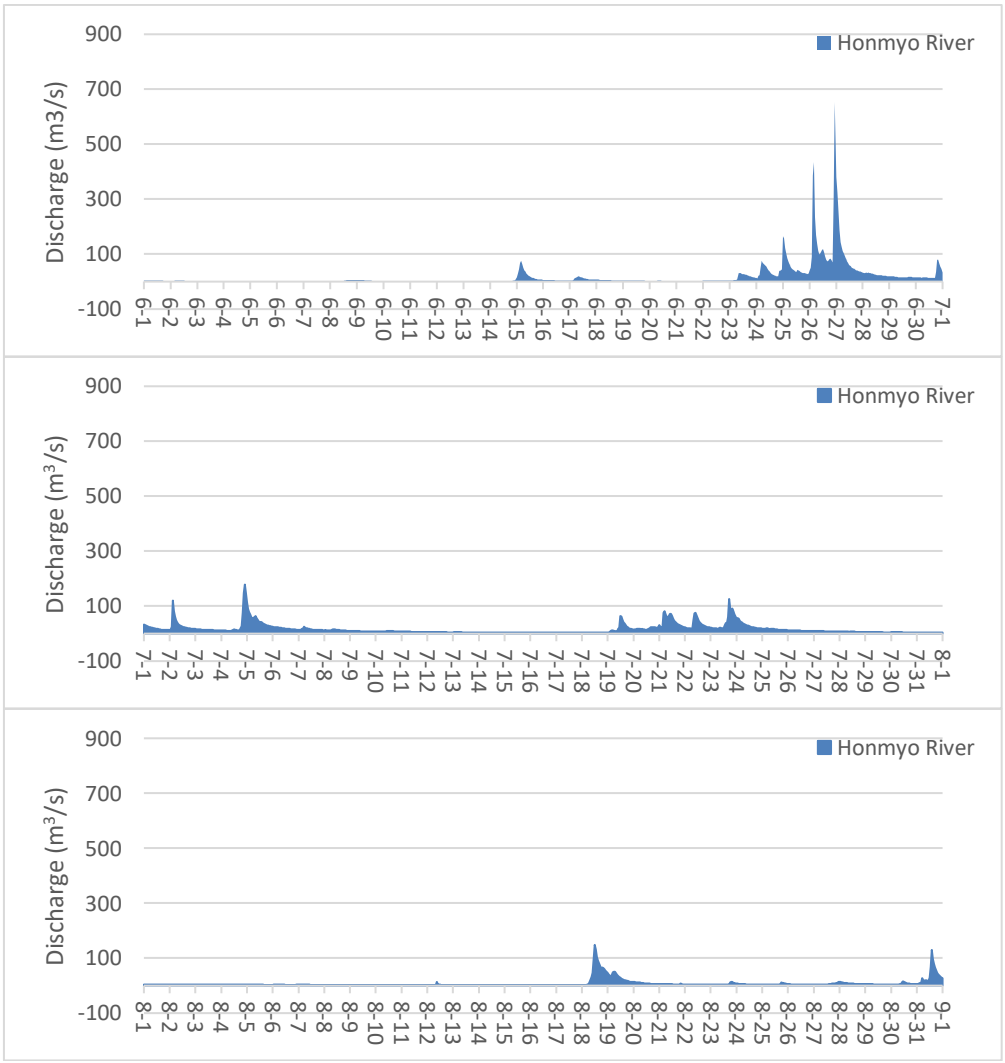

Figure 16 Hydrographs for June, July and August 2006 for the Honmyo River

Figure 17 shows the salinity at the surface layer at 14:00 on the 26th of July 2006. In the figure the computational domain for this scenario can be seen together with the lowered salinity where the rivers including the Honmyo River are discharging. At this time there was a discharge of 10.4 m^3/s from the Honmyo River. The date and time was chosen as a demonstrative example.

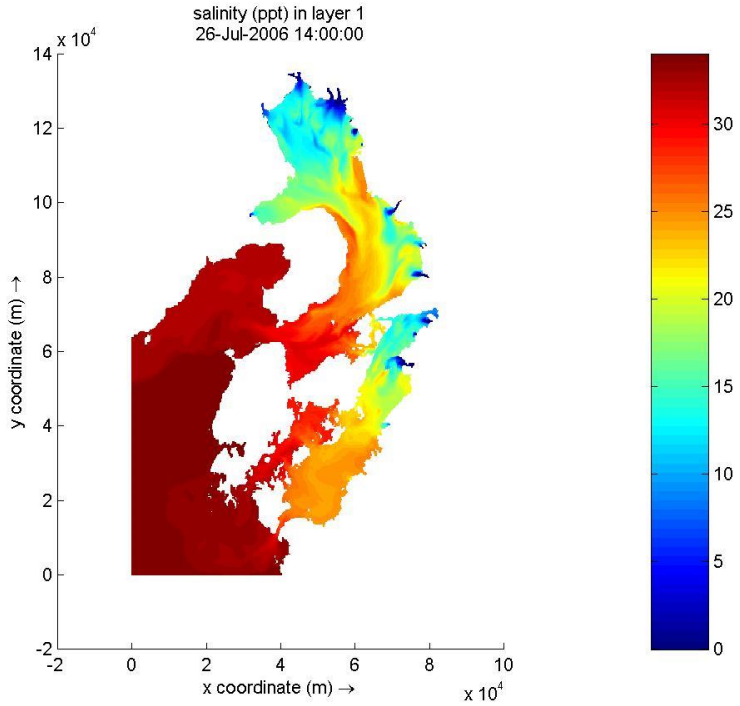

Figure 17 Scenario (1), without the dike: Computational domain and salinity at the surface layer

5.2 Scenario (2): Conditions with dike

This scenario was done to show the conditions in Ariake Sea that existed in 2006, i.e. after the Isahaya Sea dike had been built. The computational domain was used in accordance with Figure 11 but it stopped at the Isahaya Sea dike. The water area closed off by the Isahaya Sea dike, such as the Honmyo River, was not included in the computational domain. In this scenario discharge from the North Gate and the South Gate respectively (Ministry of Agriculture, Forestry and Fisheries of Japan, 2008) were used with time steps of 2mins in addition to the discharge data used in all of the scenarios.

According to the Ministry of Agriculture, Forestry and Fisheries of Japan (2008) the total water volume from the North Gate and the South Gate together were $2.55 * 10^8 m^3$ during 2006. When comparing this value to the total water volume from the Honmyo River, $1.09 * 10^8 m^3$, a difference can be seen. To be able to compare the results of the different scenarios the discharge from the North Gate and the South Gate were recalculated so that the total water volume from the two gates during the year of 2006 was equal to the total water volume from the Honmyo River during the same period. The calculations were done as follows, first a factor α was calculated

$$\alpha = \frac{V_{tot,H}}{V_{tot,N.G+S.G}}$$

where $V_{tot,N.G+S.G}$ is the total water volume in m^3 from both the North Gate and the South Gate.

α was then used to calculate the new total volume for the two gates, $V_{tot,N.G+S.G,new}$, according to the following equation

$$V_{tot,N.G+S.G,new} = \sum \alpha * V_{S.G} + \sum \alpha * V_{N.G} \quad (1.26)$$

where $V_{S.G}$ is the water volume in m^3 from the South Gate at each time step and $V_{N.G}$ is the water volume in m^3 from the North Gate at each time step.

Using equation 1.26 it could be seen that the new total water volume from the two gates were $1.09 * 10^8 m^3$, i.e. the same amount as the total water volume from the Honmyo River during the same time period, the year 2006. The discharge from the South Gate at each time step (m^3/s) that was used in the simulations, $Q_{S.G}$, was calculated with the following equation

$$Q_{S.G} = \frac{\alpha * V_{S.G}}{t_G} \quad (1.27)$$

where $V_{S.G}$ is the water volume from the South Gate at each time step in m^3 and t_G is a constant time at 120 seconds.

The discharge from the North Gate at each time step (m^3/s), $Q_{N.G}$, was then calculated using the following equation

$$Q_{N.G} = \frac{\alpha * V_{N.G}}{t_G} \quad (1.28)$$

where $V_{N.G}$ is the water volume from the North Gate at each time step in m^3.

The hydrographs for the discharge from the North Gate and the South Gate calculated in equation 1.27 and equation 1.28 can be seen in Figure 18.

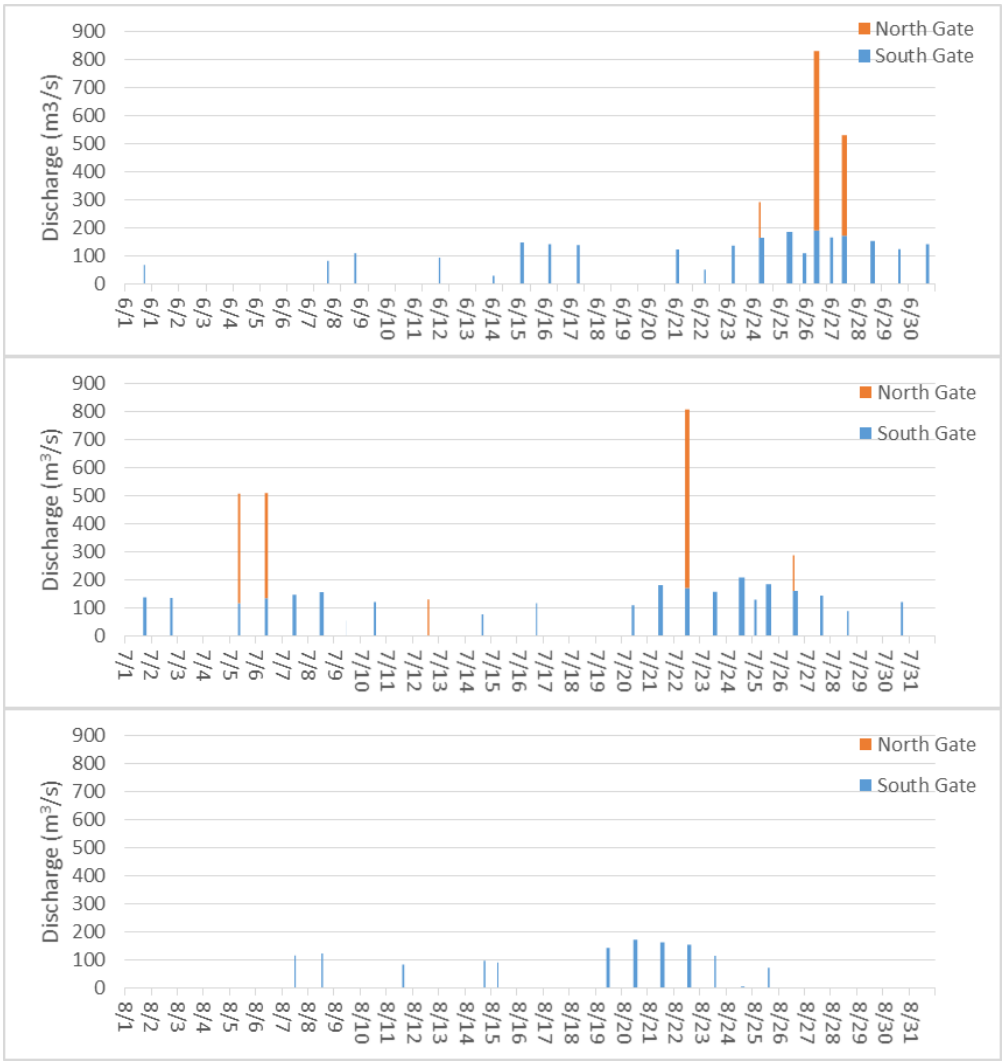

Figure 18 Hydrographs for June, July and August 2006 for the North Gate and the South Gate of the Isahaya Sea dike

Figure 19 shows the salinity at the surface layer at 14:00am on the 26th of July 2006. In the figure the computational domain for this scenario can be seen together with the lowered salinity where the rivers and gates are discharging. At this time there was a discharge of 167.36416 m^3/s from the South Gate and a discharge of 130.83393 m^3/s from the North Gate in this scenario, after adapting the discharge in accordance with the total discharge of the Honmyo River. The date and time was chosen as a demonstrative example.

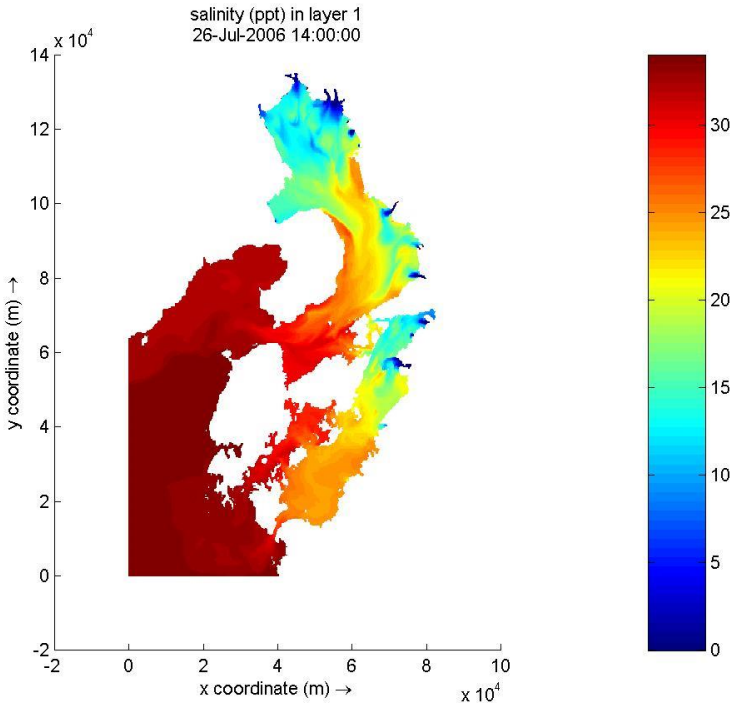

Figure 19 Scenario (2), with the dike: Computational domain and salinity at the surface layer

5.3 Scenario (3): Conditions with dike but with Honmyo River discharge from the North Gate

This scenario was conducted in order to see the effects of the spatial change of freshwater discharge. The computational domain used was the same as in scenario (2). The water area that is closed off by the Isahaya Sea dike was not included in the computational domain as it stopped at the dike. The computational domain can be seen in Figure 11. In contrast to in scenario (2) this scenario used hourly discharge from the Honmyo River in addition to the discharge data used in all of the simulations. The discharge from the Honmyo River was put as if it was discharging from the location of the North Gate and the discharge is still continuous. Table 3 shows Honmyo River catchment area, discharge and station information. Equation 1.23 was used to calculate the discharge and Figure 16 shows the hydrographs for the Honmyo River for the months of June, July and August during 2006. Figure 20 shows the salinity at the surface layer at 14:00am on the 26th of July 2006.

In the figure the computational domain for this scenario can be seen together with the lowered salinity where the rivers and the North Gate are discharging. At this time there was a discharge of 10.4 m^3/s from the Honmyo River so in this scenario there was a discharge of 10.4 m^3/s from the North Gate. There was no discharge from the South Gate during this scenario. The date and time was chosen as a demonstrative example.

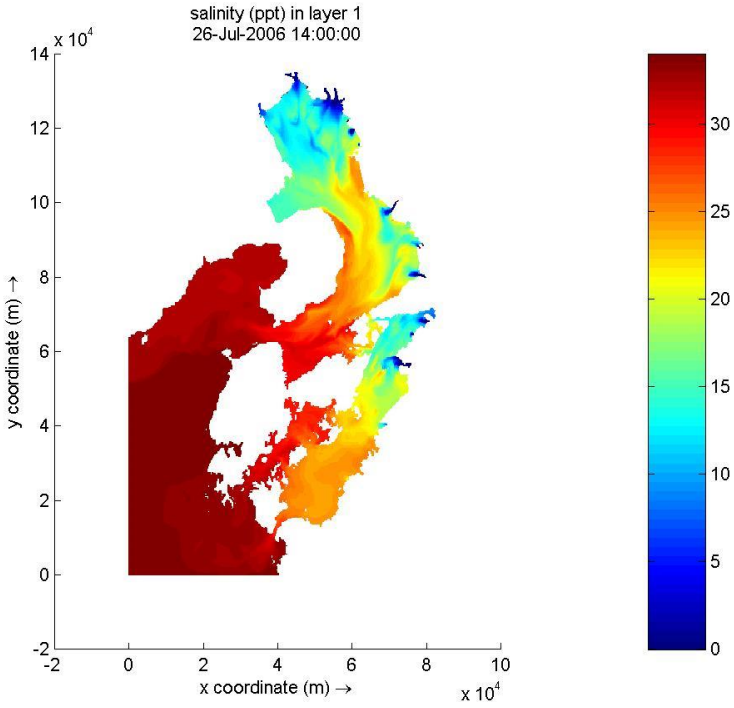

Figure 20 Scenario (3), with the dike and Honmyo River discharge from the North Gate: Computational Domain and salinity at the surface layer

6 Comparisons of different scenarios

Using the three different scenarios four comparisons were done. The first comparison is between scenario (3) and scenario (1). This means it is a comparison between the conditions that would occur if the Honmyo Rivers' discharge was moved to where the North Gate of the Isahaya sea dike is located today and the conditions that would have been if the Isahaya Sea dike had not been built before 2006. The comparison was done in order to study how the spatial change of freshwater discharge and weakened vertical mixing due to the Isahaya sea dike has affected the baroclinic structure in the Ariake Sea.

The second comparison is between scenario (2) and scenario (3). This means it is a comparison between the conditions occurring with the existing Isahaya sea dike and the conditions that would occur if the Honmyo Rivers discharge was moved to where the North Gate of the Isahaya sea dike is located today. The comparison was done in order to specifically study how the temporal change of freshwater discharge due to the Isahaya Sea Dike has affected the baroclinic structure in the Ariake Sea.

The third comparison is scenario (2) and scenario (1). This means it is a comparison between the conditions that occurred in 2006 with the existing Isahaya sea dike and the conditions that would have been if the Isahaya Sea dike had not been built before 2006. The comparison was done in order to study how the spatial change of freshwater discharge, the temporal change of freshwater discharge and the weakened vertical mixing has affected the baroclinic structure in the Ariake Sea.

The weakened vertical mixing due to the construction of the dike was further studied by comparing the results of scenario (3) – (1) and the results of scenario (2) – (1) with the results of Yano and Nishimura (2014).

A summary of the scenarios, the three first comparisons and the effects included in each comparison can be seen in Table 5.

Table 5 Summary of scenarios, comparisons and effects.

Comparison of different scenarios	**Effects**
(3)-(1) Fig. 20-23	①+ ②
(2)-(3) Fig. 24-27	③
(2)-(1) Fig. 28-31	① + ② + ③
(2)'-(1)' (Yano & Nishimura, 2014)	①
Scenarios	
(1): Without dike and with Honmyo River discharge (past conditions)	
(2): With dike and discharge from the two gates (present conditions)	
(3): With dike but with Honmyo River discharge from the North Gate.	
(1)': As in (1) but without Honmyo River discharge (Yano & Nishimura, 2014)	
(2)': As in (2) but without discharge from the two gates (Yano & Nishimura, 2014)	
Effects included in each comparison	
① Weakened vertical mixing due to the construction of the dike.	
② Change in the freshwater discharge position, spatial change from Honmyo River mouth to the two gates.	
③ Temporal change from continuous freshwater discharge to intermittency of freshwater discharge.	

The figures for these three comparisons (Figure 20-25, 29-34) have been made using exported data regarding salinity and water depth from the simulations in Delft3D for the four different points; a=B3, b=KS73-1 in the northern parts of the Ariake Sea, c=KS73-2 in the eastern part of the Ariake Sea and d=KS01-7(4) at Shimabara observation station shown in Figure 21 below.

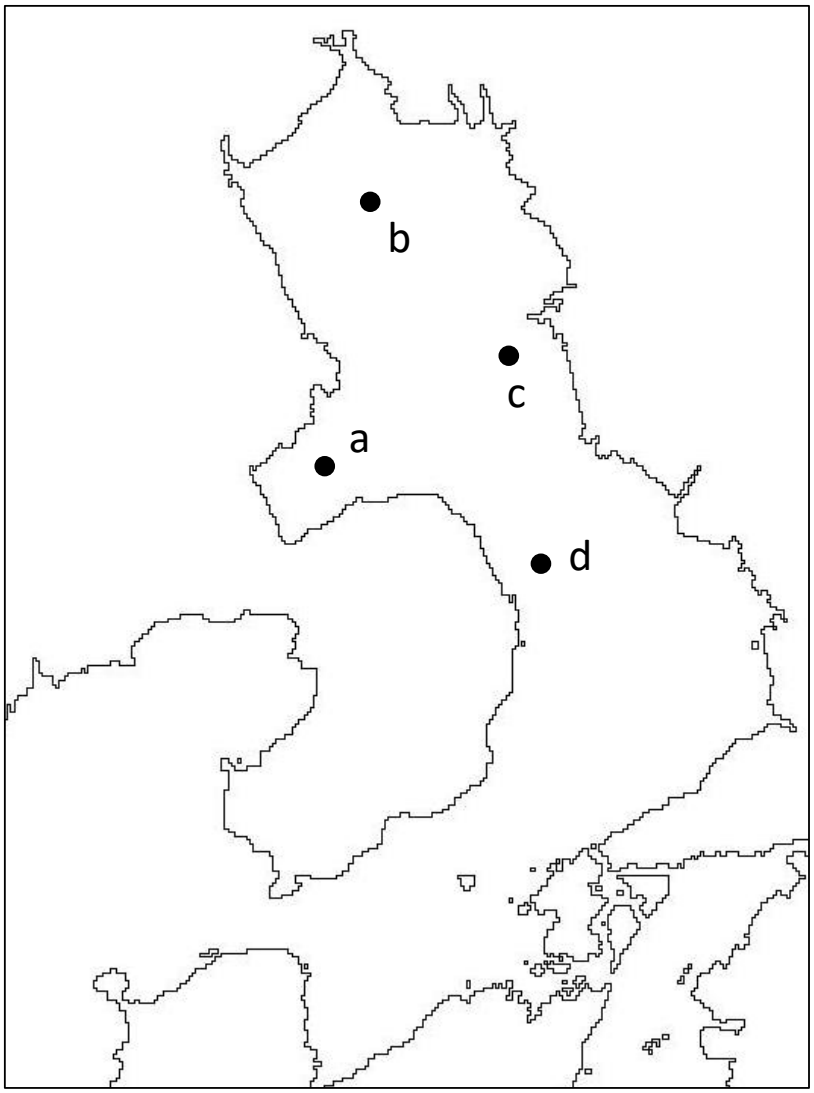

Figure 21 Four observation points (a, b, c and d) in the Ariake Sea.

Using the data from the simulations in Delft3D-FLOW the calculations were conducted with Excel. To create the figures Fortran programming language together with the program GMT, the Generic Mapping Tools, were used. The figures for these three comparisons (Figure 22-27, 31-36) show the difference in salinity at the four different observation points (Figure 21) between the compared scenarios. All of the figures (Figure 22-27, 31-36) are presented in the same way. The horizontal axis shows the time in days for the three months of June, July and August in 2006. The vertical axis shows the water depth or position from the sea bed in meters. The vertical colour spectrum to the right of the figures shows the change in salinity represented by colours. Blue areas show where the salinity has declined (negative value) in the comparison and red areas show where the salinity has increased (positive value) in the comparison. The different shades of blue or red shows how sever the difference is.

The fourth comparison was between scenario (1) and scenario (2). In contrast with the previous comparisons this is a comparison between the salinity distributions with depth at specific times in point a (Figure 21) for the two scenarios. This means that it is a comparison between the salinity distribution with depth for the conditions that would have been if the Isahaya sea dike had not been built before 2006 and the conditions occurring with the existing Isahaya sea dike. The comparison was done in order to study if there has been a change in the salinity distribution due to the construction of the dike and if stratification occurs.

6.1 Scenario (3) – scenario (1): Weakened vertical mixing and spatial change of freshwater discharge

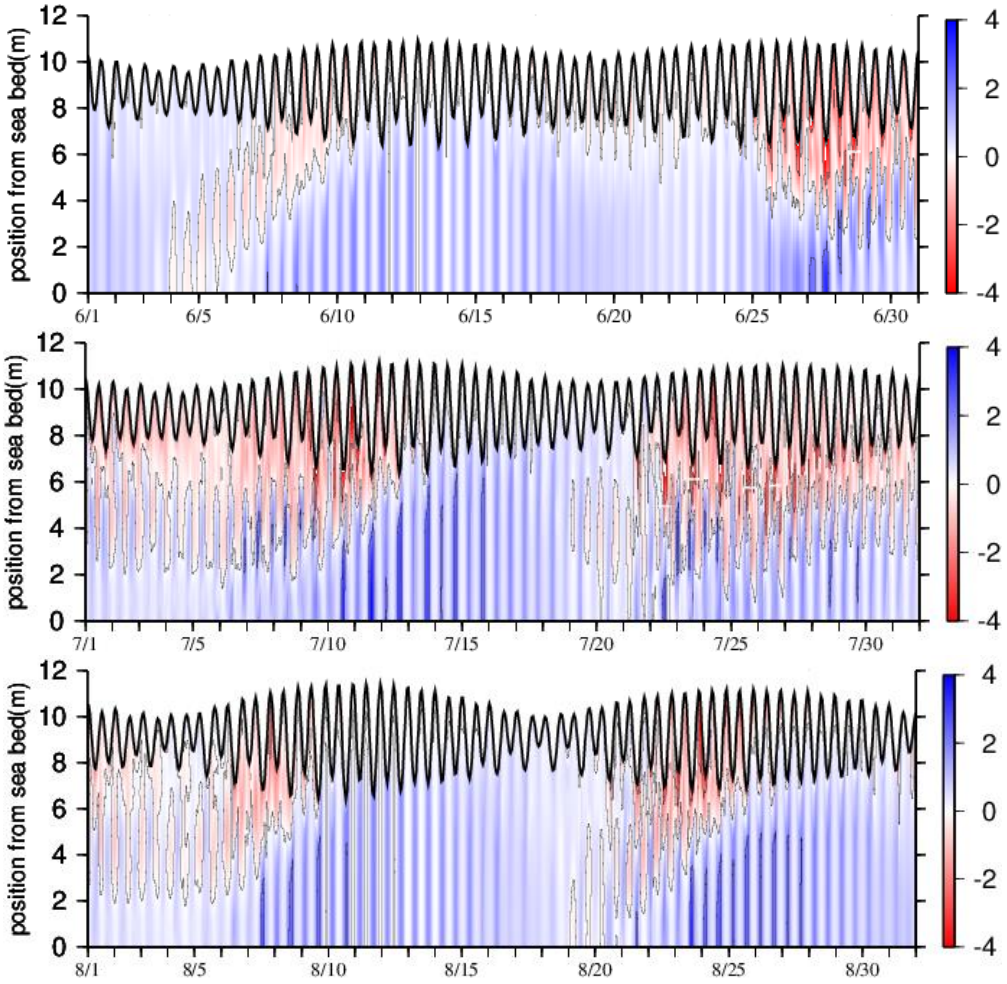

Figure 22 Amount of change in salinity at point a (scenario (3) – scenario (1))

As can be seen in Figure 22 there is a visible difference between the two scenarios in this comparison, scenario (3) and scenario (1), at point a (Figure 21), i.e. in the area inside Isahaya Bay. From Figure 22 it can be seen that a decreased salinity at the surface in scenario (3) compared to in scenario (1) occurs primarily in the change from neap tide to spring tide. It can also be seen that during these times an increased salinity at the bottom layers occurs in scenario (3) compared to scenario (1). The figure shows overall that there is a

significant influence at point a due to the weakened vertical mixing and/or change in the freshwater discharge position occurring from the building of the dike.

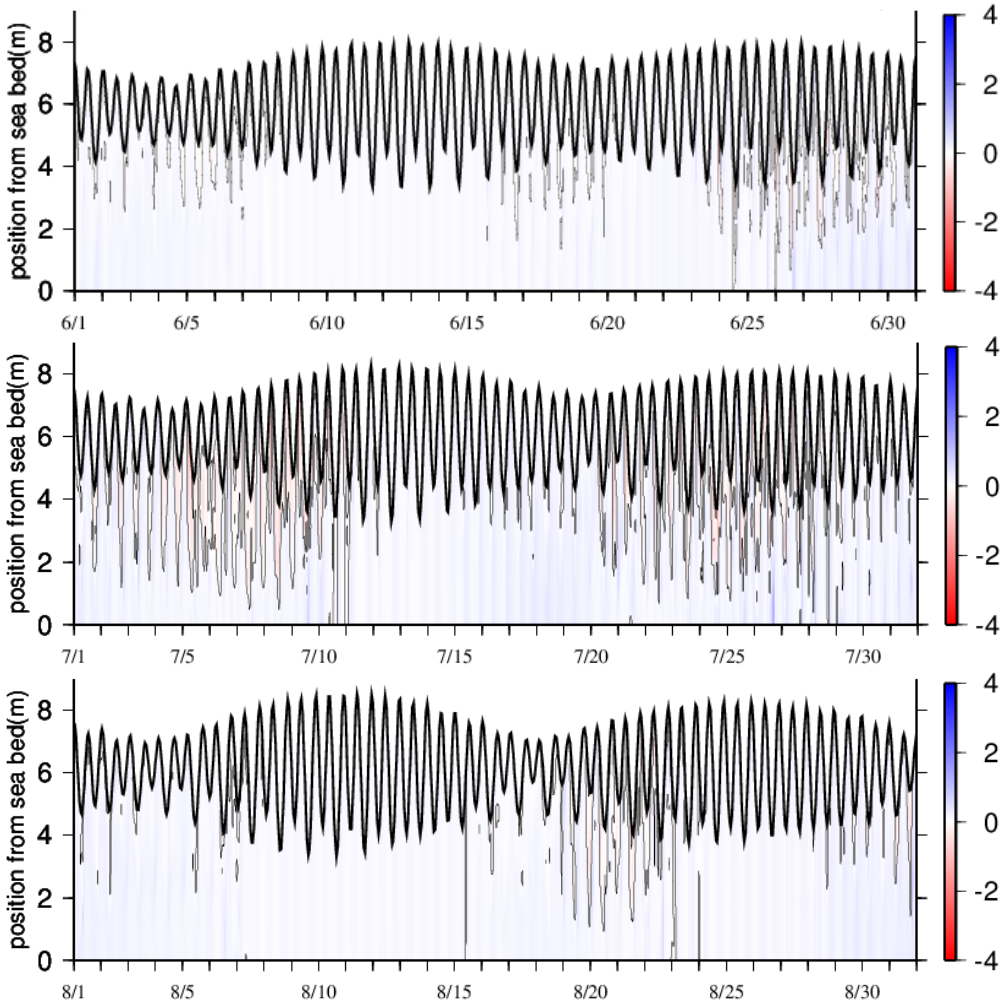

Figure 23 Amount of change in salinity at point b (scenario (3) – scenario (1))

From Figure 23 it can be seen that there is almost no difference between scenario (3) and scenario (1) at point b (Figure 21).

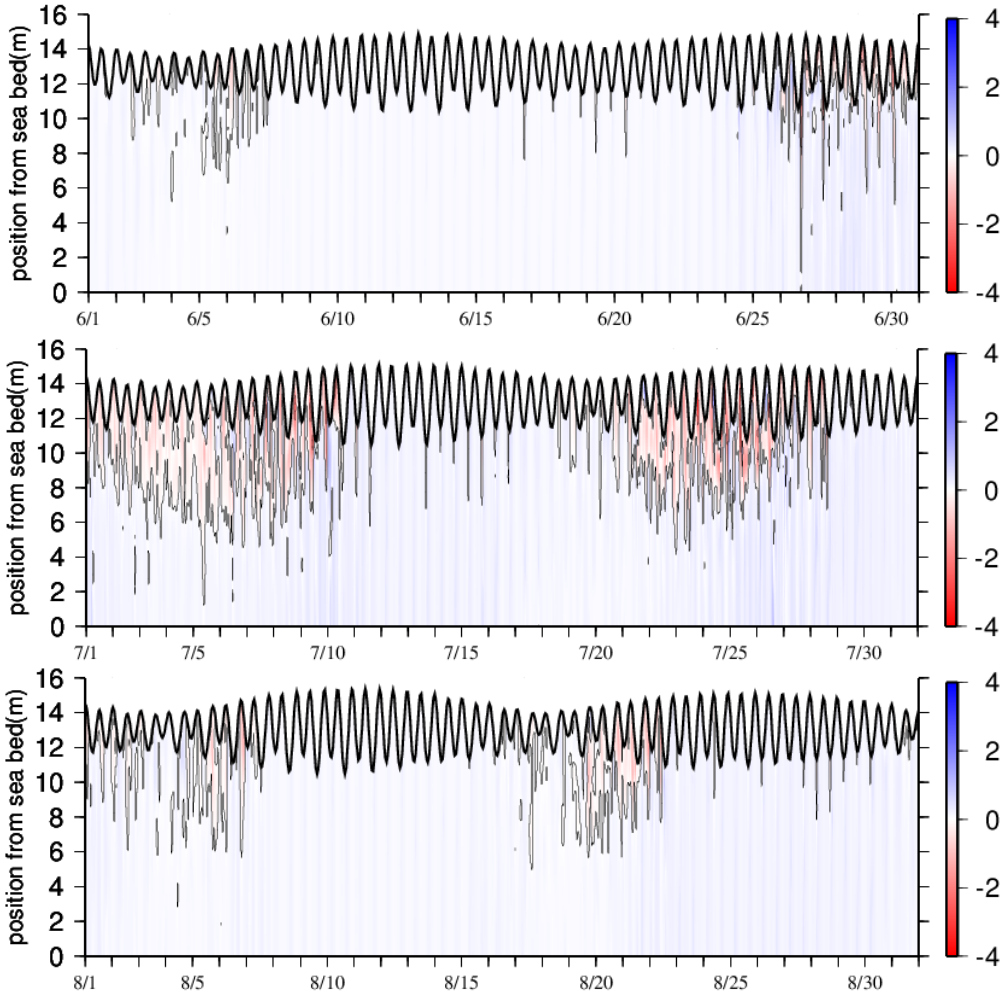

Figure 24 Amount of change in salinity at point c (scenario (3) – scenario (1))

In Figure 24 a difference in the salinity distribution between the two different scenarios can be seen at times in point c. This difference can primarily be observed in the change from neap tide to spring tide.

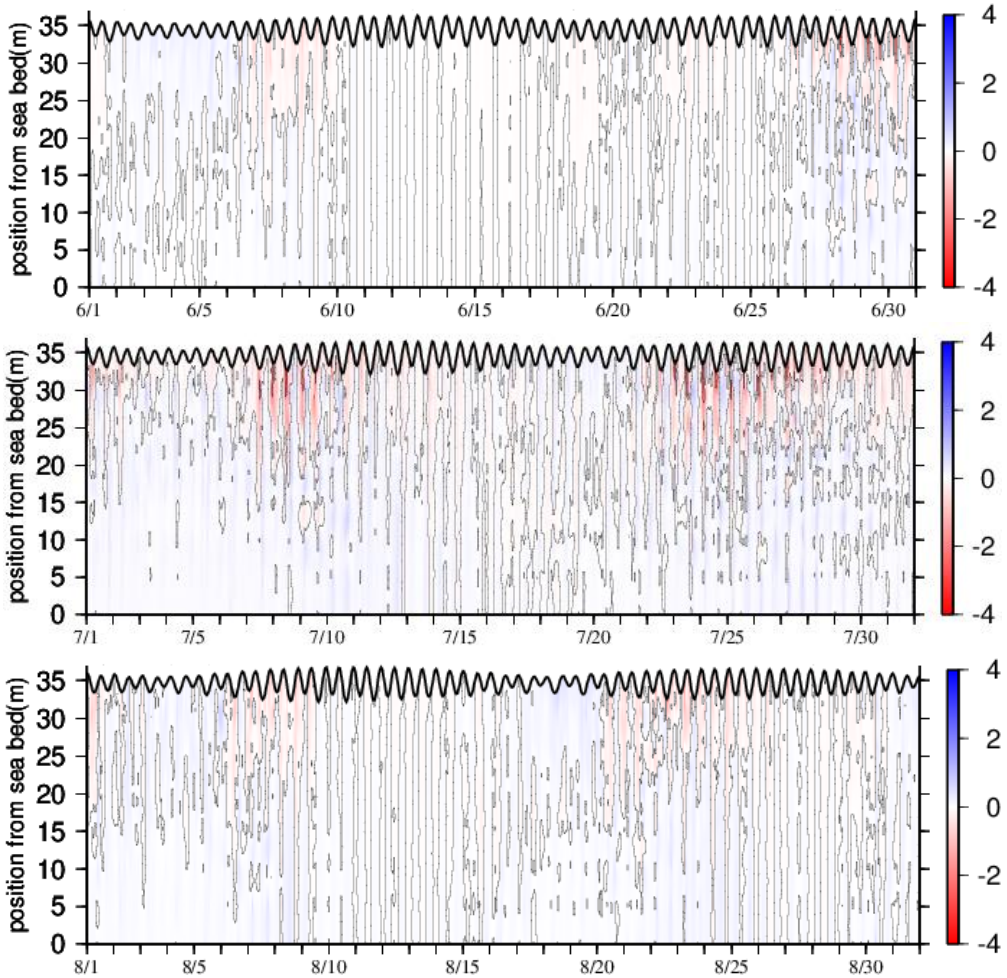

Figure 25 Amount of change in salinity at point d (scenario (3) – scenario (1))

Figure 25 shows that there is a small difference between scenario (3) and scenario (1) at point d (Figure 21). Again this difference can mainly be seen in the change from neap tide to spring tide. In this figure it can also be seen a difference between July and the other two months.

6.2 Scenario (2) – Scenario (3): Temporal change of freshwater discharge

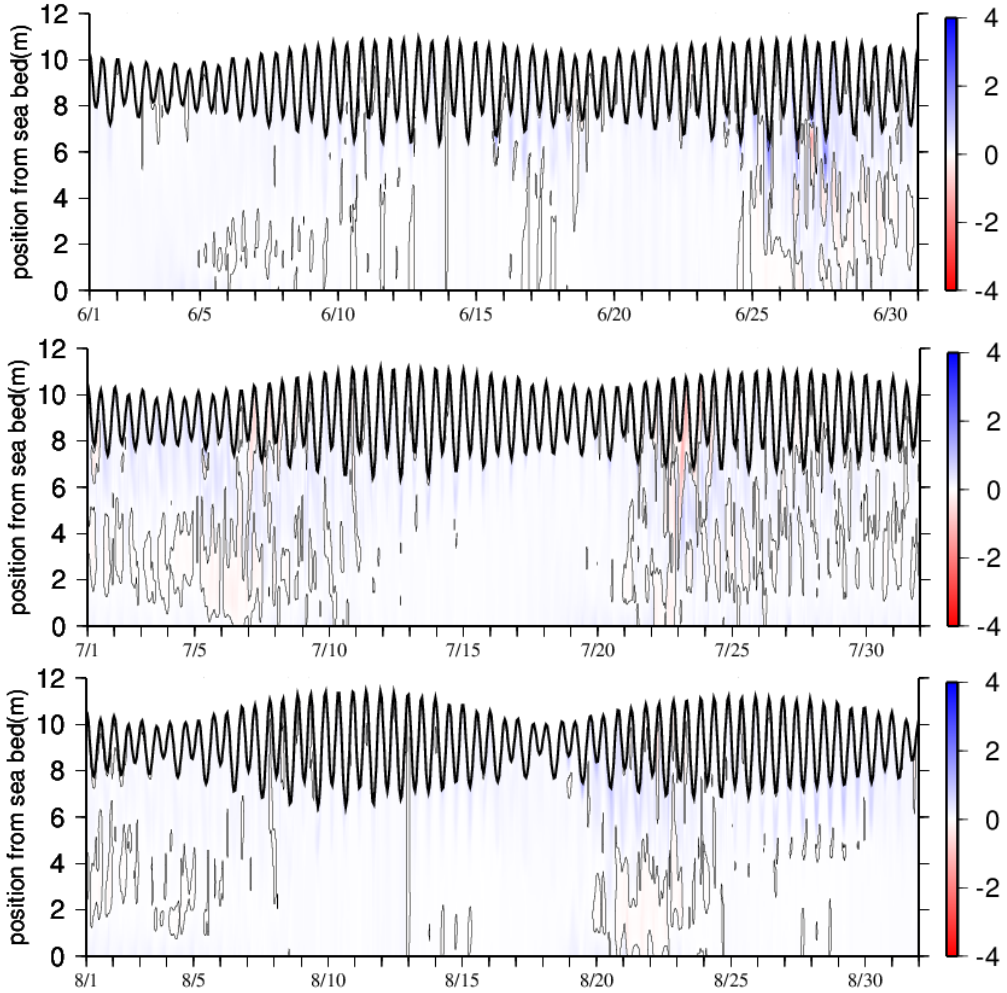

Figure 26 Amount of change in salinity at point a (scenario (2) – scenario (3))

From Figure 26 it can be seen that the temporal change of freshwater discharge from continuous to intermittent flow has caused no change at point a (Figure 21). The figures for points b, c and d can be found in appendix due to that none of them show any difference between the scenario (2) and scenario (3).

6.3 Scenario (2) – Scenario (1): Weakened vertical mixing, spatial and temporal change of freshwater discharge

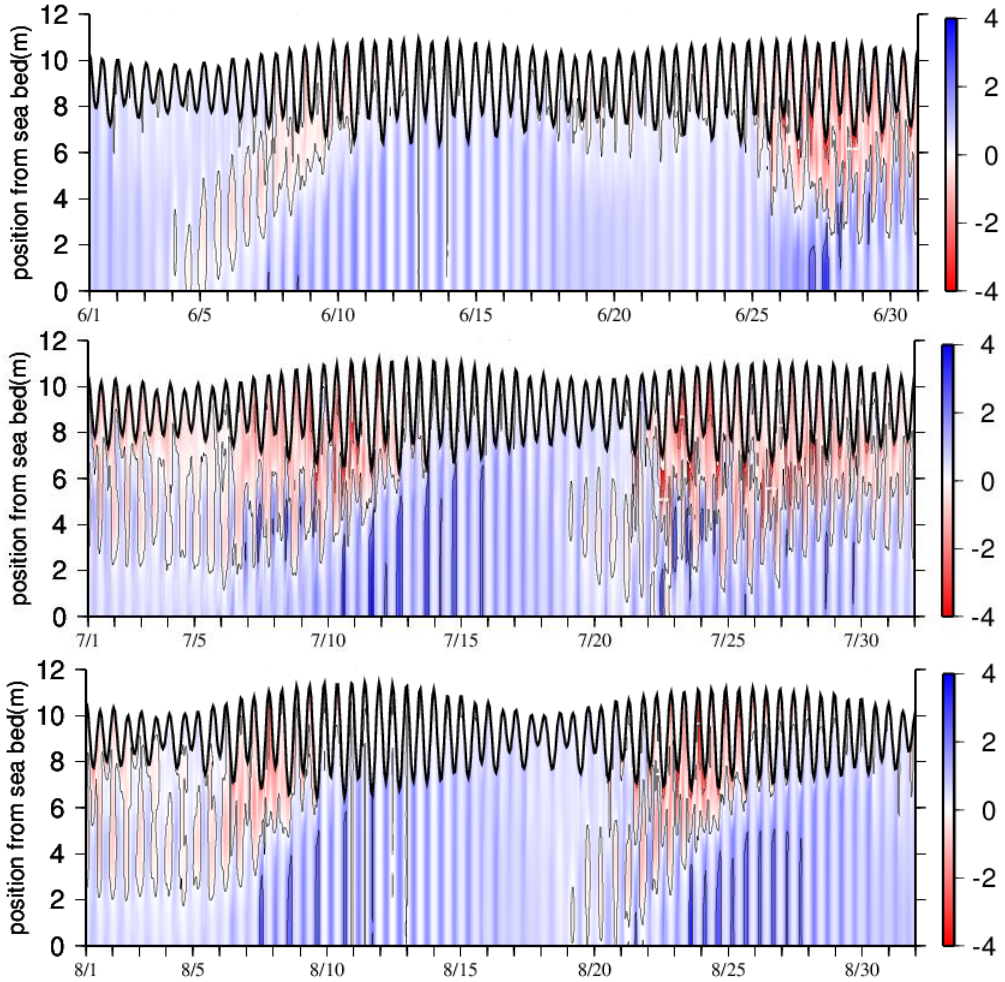

Figure 27 Amount of change in salinity at point a (scenario (2) - scenario (1))

When combining the influence from the spatial change and the influence from the temporal change of freshwater discharge it can be seen that Figure 27 is very similar to Figure 22. Due to that the figures for points b, c and d in this comparison are also very similar to Figures 22-25 which are for points b, c, and d in the comparison between scenario (3) and scenario (1) they have been put in the appendix.

6.4 Scenario (1) and scenario (2): Salinity distribution with depth

Figure 28-30 show the salinity distribution with depth at specific dates and times for scenario (1) and scenario (2). The comparison was done for point a (Figure 21) because the biggest difference between the scenarios could be seen in Figure 27. The times in the figures (Figure 28-30) were chosen due to that these times showed big differences in the salinity distribution during neap tide, during the transition from neap tide to spring tide and during spring tide respectively. Figure 28 shows the salinity distribution with depth during neap tide and high tide on the 4th of July 2006 at 21:00. On the left the figure shows the salinity distribution for scenario (1) and on the right the salinity distribution for scenario (2). As can be seen in the figure there is a slightly bigger difference between the salinity at the bottom and the salinity at the surface in the results of scenario (2) compared to the results of scenario (1). Figure 29 shows the salinity distribution with depth during the transition from neap tide to spring tide, but still close to neap tide, and low tide on the 22nd of July 2006 at 13:00. On the left the figure shows the salinity distribution for scenario (1) and on the right the salinity distribution for scenario (2). As can be seen in the figure there is a large difference in the salinity distribution of scenario (2) compared to the salinity distribution of scenario (1). Figure 30 shows the salinity distribution with depth during spring tide and low tide on the 27th of June 2006 at 16:00. On the left the figure shows the salinity distribution for scenario (1) and on the right the salinity distribution for scenario (2). From the figure it can be seen that there is a large difference between the salinity at the bottom and the salinity at the surface in the results of scenario (2) whereas there is only a small difference in the results of scenario (1).

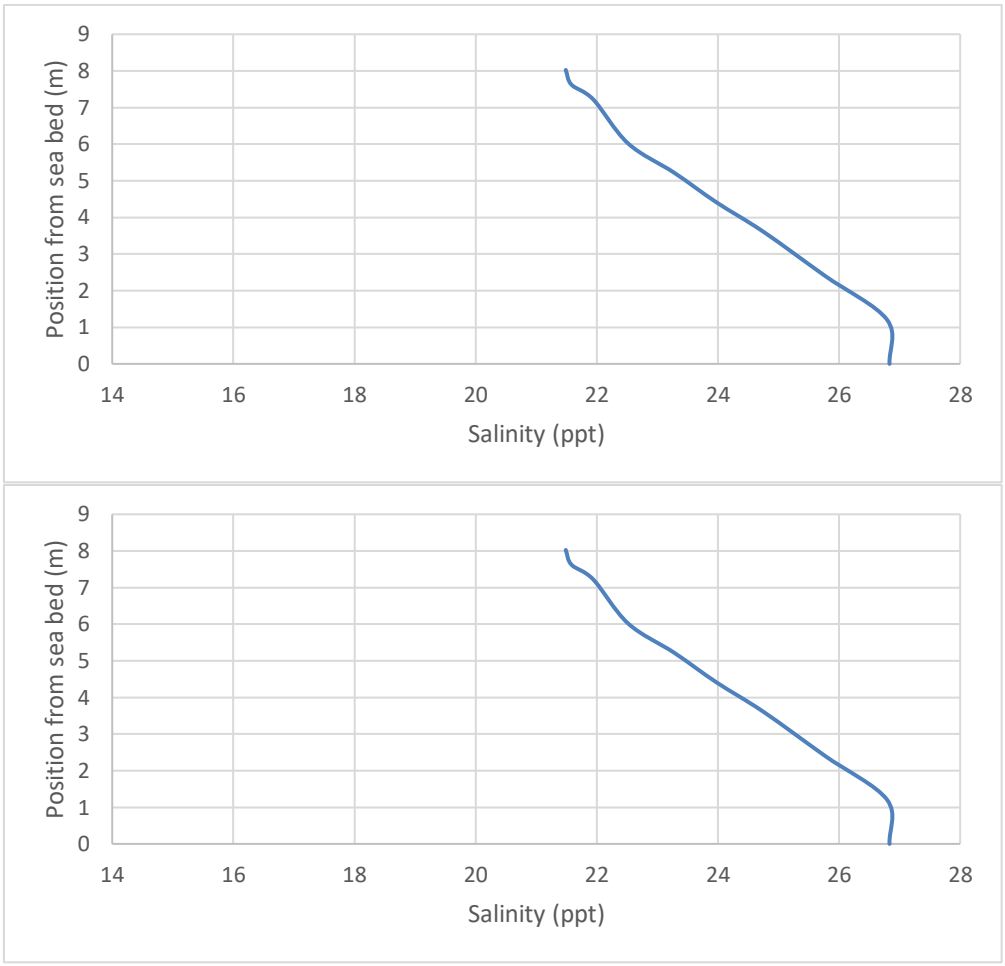

Figure 28 Salinity distribution with depth on the 4th of July 2006 at 21:00 for scenario (1) above and scenario (2) below

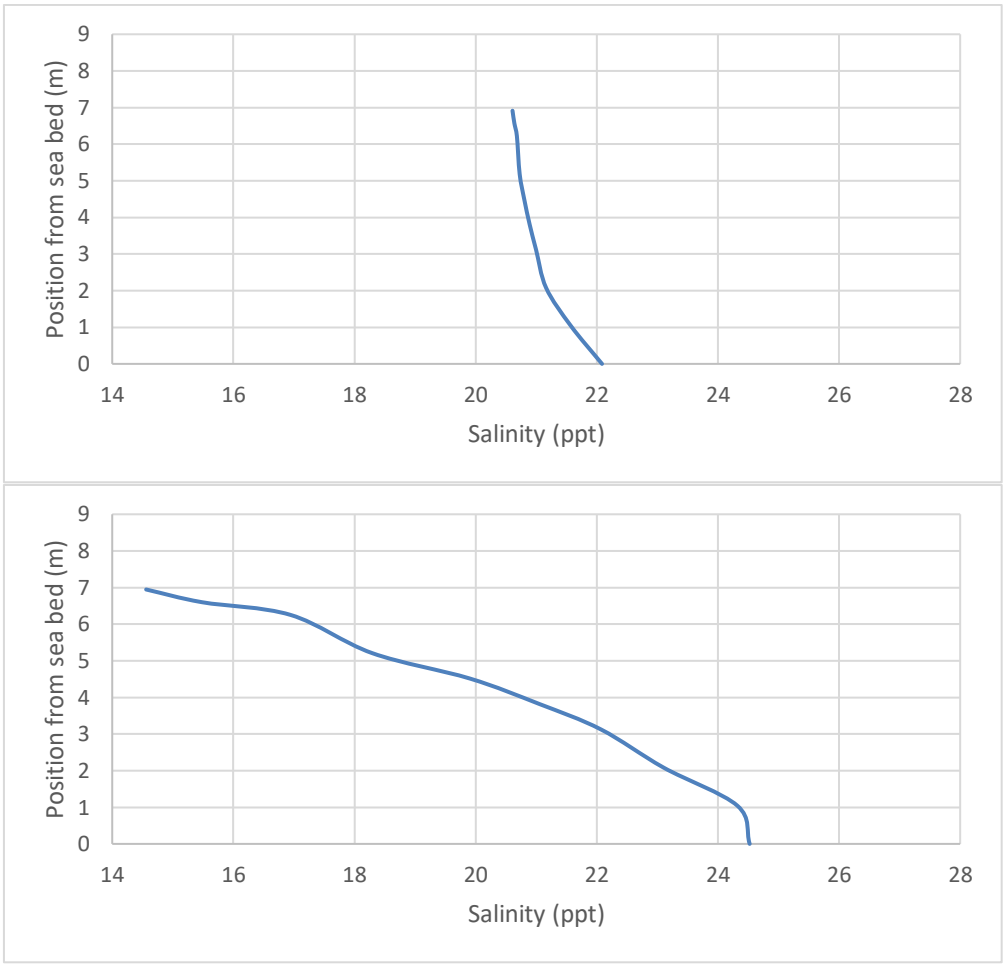

Figure 29 Salinity distribution with depth on the 22nd of July 2006 at 13:00 for scenario (1) above and scenario (2) below

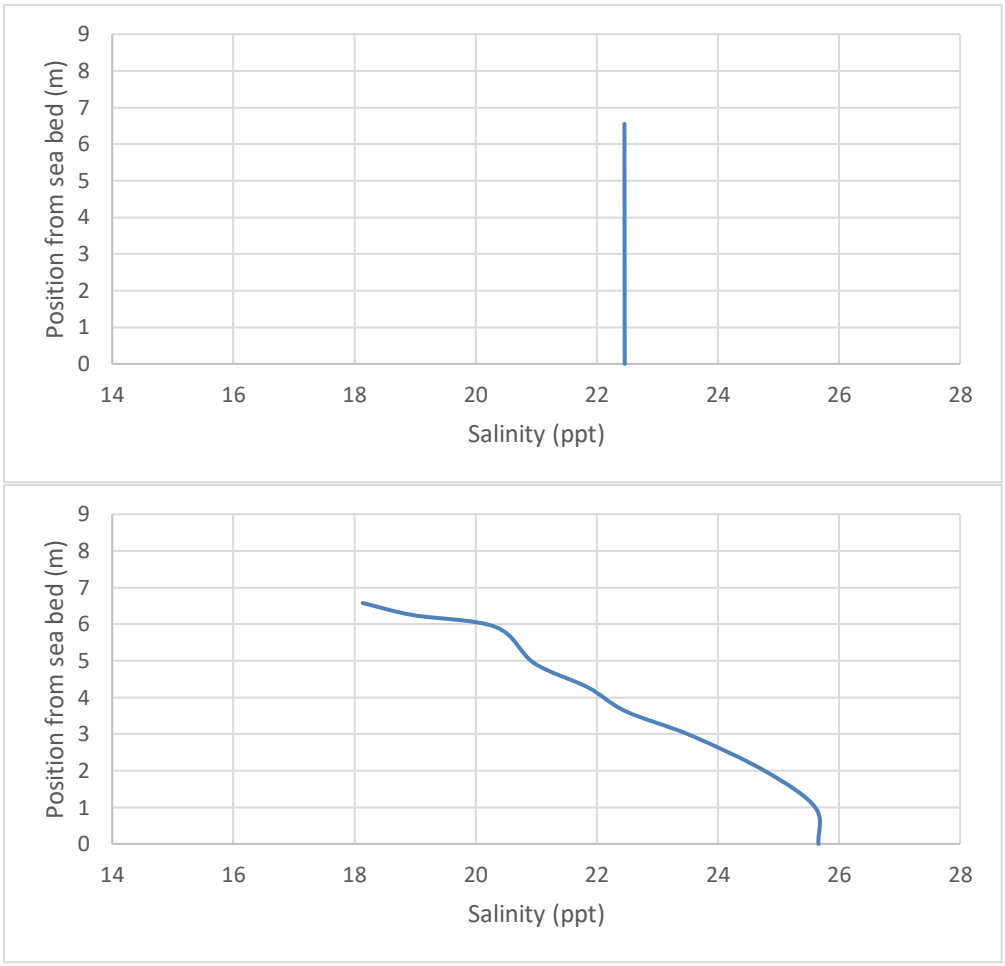

Figure 30 Salinity distribution with depth on the 27th of June 2006 at 16:00 for scenario (1) above and scenario (2) below

7 Discussion

Before Yano and Nishimura (2014) did their study "Numerical Analysis on the effect of large reclamation on the baroclinic structure in the Ariake Sea, Japan" the effect of the dike on stratification and baroclinic structure had not been studied. There had only been related studies, e.g. regarding water exchange and estuarine circulation (Yanagi & Abe, 2003; Yanagi & Abe, 2005; Yanagi & Shimomura, 2006), and flow of freshwater from the Chikugo River (Yamaguchi & Hayami, 2009). In the study by Yano and Nishimura (2014) they did not take into account the freshwater discharge from the Honmyo River or from the North Gate and South Gate of the Isahaya Sea Dike. Whether including this discharge would change the result of Yano and Nishimura (2014) regarding weakened vertical mixing due to the construction of the Isahaya Sea Dike has therefore not been studied before. In addition, how the changes to the freshwater discharge, both spatial and temporal, due to the sea dike has affected the baroclinic structure has not previously been studied in detail.

7.1 Comparisons of different scenarios

In Figures 22 – 27 regarding "Amount of change in salinity" it can be seen that the effect of the Isahaya Sea Dike is not constant at all times, i.e. the effect changes over time in the comparisons. It could be seen that the effect is stronger during the transition from neap tide to spring tide, and during spring tide than it is during neap tide. This, however, does not mean that the effect that occurs during neap tide is necessarily less important than the bigger effects during the transition from neap to spring tide, and during spring tide. The reason is that during neap tide the water column is more easily stratified than during spring tide due to less mixing power (Simpson & Sharples, 2012). This difference is because the velocity of the water is small during neap tide whereas it is large during spring tide. Due to that the velocity of the water is already small during neap tide and the water column is more easily stratified even a small change in stratification during neap tide would be more likely to lead to hypoxic bottom water than the same change in stratification during spring tide. So the difference in stratification during neap tide when comparing scenario (1), the conditions before the dike was built, with scenario (2), the conditions after the dike was built, Figure 27, might not need to be big to make an impact on the environment. In contrast the difference of water velocity between scenario (1), the conditions before the construction of the dike, and scenario (2), the conditions after the construction of the dike, during spring tide might

be large without causing a change in the stratification because the original velocity was large. Following a similar reasoning to that regarding neap tide, a change in stratification might need to be large during spring tide to make a difference on the environment or cause hypoxic conditions to develop. So even though the effect of the sea dike differs between neap tide, the transition from neap tide to spring tide, and spring tide it might still be important to look at all of them. Figures 22 – 27 also show that the effect of the Isahaya Sea Dike does not only follow the neap and spring tide cycle. When comparing with the hydrograph for the A-class rivers discharging into the Ariake Sea (Figure 13-15) it can be seen that the effect appears to be connected to when larger amounts of freshwater is discharging into the Ariake Sea.

The general discharge pattern of the different rivers into the Ariake Sea is that the Chikugo River has the largest freshwater discharge (Ministry of Land, Infrastructure, Transport and Tourism of Japan, 2015). However at times the discharge can be larger from other rivers such as the Kikuchi River (Figure 13-15). Due to that different rivers have different locations of the river mouths the freshwater discharge from different rivers will have different effects. The time before it enters into the Isahaya Bay will therefore also differ. A longer distance leads to a longer time lag. The amount or the part of the total river discharge that enters into the Isahaya Bay will also differ depending on the river. To understand a complete pattern of the relationship between river input and flow more simulations would be needed. For example a numerical experiment could be conducted so that a virtual situation is created, possibly where only the freshwater from the Chikugo River was considered.

7.1.1 Spatial change of freshwater discharge

The results of Yano and Nishimura (2014) are very similar to the results in the comparison between scenario (3) and scenario (1), Figures 22-25, and scenario (2) and scenario (1), Figures 27 and 34-37 (appendix). This indicates that the change in the freshwater discharge position, spatial change, does not have an effect. It is, however, difficult to determine this result for certain due to it not being possible to separate from the effect of the weakened vertical mixing. The effects do not add linearly to each other, the addition is nonlinear, and therefore the results cannot be separated exactly only approximately from looking at the figures. Even though that is the case, when looking at the strong similarities between the figures it can be roughly estimated that the spatial change does not have an effect.

7.1.2 Temporal change of freshwater discharge

The change from continuous discharge of freshwater, scenario (3), to intermittent discharge, scenario (2), did not show an effect on the salinity distribution in any of the four points studied in the Ariake Sea and the Isahaya Bay, Figure 26 and 31-33 (appendix). The reason for this could be that the amount of freshwater discharged from the Honmyo River and the dikes' two gates is not large enough to show an effect. The amount of freshwater flowing into the Isahaya Bay from other A-class rivers, such as the Chikugo River, could be more important. To study this one way could be to compare the input of freshwater from other rivers' input into the Isahaya Bay with the freshwater discharge from the dikes' two gates and the Honmyo River. It would be easy to obtain the information regarding the freshwater discharged from the two gates and the Honmyo River but only a part of the freshwater discharged from the other rivers flow into the Isahaya Bay so new calculations might be necessary. The ratio of river inflow from rivers into Isahaya Bay could also change temporarily for example due to changes in tides. Another way to confirm the reason could be to consider a longer time period. In this comparison only 2006 was taken into consideration but a longer time period, for example 15 years, might be needed to discover more certain patterns. By doing a longer study many different conditions might occur so that the results could be summarized.

7.1.3 Weakened vertical mixing

Since the previous research (Yano & Nishimura, 2014) omitted the freshwater discharge from the Honmyo River and from the two gates of the Isahaya Sea Dike and since the results, Figure 22 and Figure 27, are very similar it is indicating that the freshwater discharge from Honmyo River and from the gates are not important whereas the weakened vertical mixing is. This is however only in point a, Figure 21, since for points b, c and d none of the comparisons showed any significant change, Figures 23-25 and Figures 34-36 (appendix).

7.1.4 Salinity distribution with depth

Figures 28-30 does not show any two layer system, i.e. strong stratification and likely effect on development of hypoxia. Weak or moderate stratification can, however, also affect development of hypoxia. Due to that dissolved oxygen has not been included in this study the cause of the development of hypoxia in the Ariake Sea cannot be concluded. To determine the cause further studies are needed. The development of hypoxia can in addition to the studied hydrodynamic conditions be affected by bottom sediment quality, water

quality, phytoplankton and concentration of nutrients. For example according to Hamada et al. (2008) it is possible that the reason Ariake Sea becomes more hypoxic is due to that the content of organic matter in the mud has increased. Further studies could therefore be to evaluate the conditions in the Ariake Sea by an ecosystem model.

7.2 Model simulation for different scenarios

It could be that the year studied was not representative for the Isahaya Bay and the Ariake Sea. In 2006 a record breaking hypoxia began forming in early July, reaching a maximum size in early August when it covered all the inner area of the Ariake Sea (Hamada, et al., 2008). According to Hamada, et al. (2008) the bottom DO level was, in 2006, the lowest in spring tide since 1972. In July 2006 there was also a very large river discharge which caused stratification and lead to severe hypoxia in the bottom waters (Hamada, et al., 2008). In 1980 almost identical river discharge levels and conditions of stratification occurred as in 2006 but when comparing the two different years the DO level at the bottom was lower in 2006 (Hamada, et al., 2008). Also in 2006 on 18-19 of August 2006 the Ariake Sea was hit by a storm and as a consequence flooding occurred on 18-21 of August in the head of the Ariake Sea (Nakata, et al., 2010). According to Nakata et al. (2010) during the offshore wind the bottom water tends to intrude into Isahaya Bay. Due to this movement the bottom water in the Isahaya Bay increased in density and the DO level of the water decreased (Nakata, et al., 2010). The stratification in 2006 could be increased by the combination of high density bottom water entering the Isahaya Bay together with the low density water at the surface due to the flooding (Nakata, et al., 2010). These are all specific conditions for 2006 which might not be common during other years. It might therefore be good to further study how the Isahaya Sea Dike has affected the baroclinic structure in the Ariake Sea during other years or over a longer period. It could further be that point a, Figure 21, is not representative for Isahaya Bay so that other points inside the bay might be affected more or less by the construction of the Isahaya Sea Dike. Further studies could therefore be to look at different points inside the Isahaya Bay to determine whether point a is a representative point for the bay.

To be able to compare the three different scenarios the total freshwater discharge from the sea dike's two gates were recalculated so that the total was the same as the total for the Honmyo River discharge. The difference in the amount of discharge from the Honmyo River compared with from the two gates could be due to that there is discharge into the inner pond of the Isahaya sea dike from not only Honmyo River but also from other small rivers and drains. These small rivers and drains have not been accounted for when doing the simulation without the Isahaya sea dike.

8 Conclusions

The results presented in this report suggest that the spatial change of freshwater discharge due to the construction of the Isahaya Sea Dike, from the Honmyo River mouth to the two gates of the sea dike, has not affected the baroclinic structure in the Ariake Sea. It was further shown that the baroclinic structure in the Ariake Sea has not been affected by the temporal change of freshwater discharge due to the construction of the sea dike, from continuous Honmyo River discharge to intermittent sea dike discharge. The results were very similar to the results of Yano and Nishimura (2014) regarding vertical mixing. Their results of weakened vertical mixing due to the construction of the sea dike could therefore be confirmed. Further studies with water and bottom sediment qualities are needed to conclude how the sea dike has affected the development of hypoxic waters in the Ariake Sea.

References

Azhikodan, G. & Yokoyama, K., 2015. Temporal and Spatial Variation of Mixing and Movement of Suspended Sediment in the Macrotidal Chikugo River Estuary.
Journal of Coastal Research, 31(3), pp. 680-689.

Cao Don, N. et al., 2007. Sediment Transport and Short-term Sedimentation Processes in the Tidal Flats of the Ariake Sea, West Coast of Kyushu, Japan. *Journal of Coastal Research,*
pp. 837-841.

Deltares, 2006. *Delft3D-FLOW User Manual, ver. 3.14.* Delft

Egbert, G. D., Ray, R. D. & Bills, B. G., 2004. Numerical modeling of the global semidiurnal tide in the present day and in the last glacial maximum. *Journal of Geophysical Research,* 109(C3003).

Fujiwara, T., Sanford, L. P., Nakatsuji, K. & Sugiyama, Y., 1997. Anti-cyclonic circulation driven by the estuarine circulation in a gulf type ROFI. *Journal of Marine Systems,* 12(1-4), pp. 83-99.

Gerritsen, H. et al., 2008. *Validation Document Delft3D-FLOW.* s.l.:Deltares.

Hamada, T. et al., 2008. Serious Hypoxia in the Head of the Ariake Sea in Summer, 2006. *Oceanography in Japan,* pp. 371-377
(in Japanese with English abstract).

Hayami, Y. & Hamada, T., 2015. Isahaya Bay, freshwater lake to an estuary again. *Marine Pollution Bulletin.*

Hiramatsu, K., Shikasho, S. & Mori, K., 2005. Numerical prediction of suspended sediment concentrations in the Ariake Sea, Japan, using a time-dependent sediment resuspension and deposition model. *Paddy Water Environ,* pp. 13-19.

Ishizaka, J., 2003. Detection of red tide events in the Ariake sound、Japan. *Proc. SPIE 4892, Ocean Remote Sensing and Applications,* pp. 264-268.

Ishizaka, J. et al., 2006. Satellite Detection of Red Tide in Ariake Sound, 1998-2001.
Journal of Oceanography, pp. 37-45.

Japan Meterological Agency a, *General Information on Climate of Japan.* [Online]
Available at:
http://www.data.jma.go.jp/gmd/cpd/longfcst/en/tourist.html
[Accessed 12 10 2015].

Japan Meterological Agency b, n.d. *Climate of the Kyushu (North) district.* [Online]
Available at:
http://www.data.jma.go.jp/gmd/cpd/longfcst/en/tourist/file/Northern_Kyushu.html
[Accessed 12 10 2015].

Japan Meterological Agency c, n.d. *Tables of Climatological Normals (1981-2010).* [Online]
Available at:
http://www.data.jma.go.jp/obd/stats/data/en/normal/normal.html
[Accessed 13 11 2015].

Kiyomoto, Y. et al., 2008. Long-term Increasing Trend of Transparency and its Relaionships to Red Tide Outbreaks in Ariake Bay. *Oceanography in Japan*, pp. 337-356
(in Japanese with English abstract).

Manda, A. & Matsuoka, K., 2006. Changes in Tidal Currents in the Ariake Sound Due to Reclamation. *Estuaries and Coasts*, pp. 645-652.

Mellor, G. L. & Blumberg, A. F., 1985. Modeling Vertical and Horizontal Diffusivities with the Sigma Coordinate System. *Monthly Weather Review*, 113(8), pp. 1379-1383.

Ministry of Agriculture, Forestry and Fisheries of Japan, 2008. [Online] Available at: http://www.isahaya-higata.net/sp/080612nousui.pdf [Accessed 1 Dec. 2015].

Ministry of Land, Infrastructure, Transport and Tourism of Japan, 2015. *Water Information System, 水文水質データベース (in Japanese).* [Online] Available at: http://www1.river.go.jp/ [Accessed 1 Dec. 2015].

Nakata, H., Mishina, H., Takahashi, T. & Hirano, K., 2010. A Newly Emerging Environmental Issue: Development of Hypoxia in the Bottom Water of Ariake Bay. *Coastal Environmental and Ecosystem Issues of the East China Sea,* pp. 1-12.

Nishimura, K., Hisano, A., Yano, S. & Tai, A., 2013. Numerical Analysis on Dynamics of Freshwater Transport from the Chikugo River in the Ariake Sea. *Proc. of the 68th Annual Meeting of JSCE, CD-ROM,* pp. pp. II-283-II-284
(In Japanese).

Phillips, N. A., 1957. A coordinate system having some special advantages for numerical forecasting. *Journal of Meteorology,* Volume 14, pp. 184-185.

Pinet, P. R., 2003. *Invitation to Oceanography.* Sudbury, MA, USA: Jones & Bartlett Learning.

Saita, T. et al., 2008. Behavior of Freshwater from the Chikugo River in the Ariake Bay. *Annual Journal of Hydraulic Engineering, JSCE,* Volume 52, pp. 1327-1332
(In Japanese with English abstract).

Simpson, J. H., 1997. Physical processes in the ROFI regime. *Journal of Marine Systems,* 12(1-4), pp. 3-15.

Simpson, J. H. & Sharples, J., 2012. *Introduction to the Physical and Biological Oceanography of Shelf Seas.* Cambridge, United Kingdom: Cambridge University Press.

Suzuki, K. W., Kanematsu, Y., Nakayama, K. & Tanaka, M., 2014. Microdistribution and feeding dynamics of Coilia nasus (Engraulidae) larvae and juveniles in relation to the estuarine turbidity maximum of the macrotidal Chikugo River estuary, Ariake Sea, Japan. *Fisheries Oceanography,* 23(2), pp. 157-171.

Takahashi, T., Umehara, A. & Tsutsumi, H., 2014. Diffusion of microcystins (cyanobacteria hepatotoxins) from the reservoir of Isahaya Bay, Japan, into the marine and surrounding ecosystems as a result of large-scale drainage. *Marine Pollution Bulletin,* 89(1-2), pp. 250-258.

Talley, L. D., Pickard, G. L., Emery, W. J. & Swift, J. H., 2011. *Descriptive Physical Oceanography: An Introduction.* Sixth ed. s.l.:Elsevier Ltd..

The Oceanographic Society of Japan, 2005. *For Rehabilitation of Ecosystem in the Ariake Sea.* Kouseisya Kouseikaku: 211p.
(In Japanese).

Tsutsumi, H. et al., 2003. Studies of the Cross Section of Water in the Innermost Areas of Ariake Bay with the Recent Occurrence of Hypoxic Water and Red Tide. *Oceanography in Japan,* pp. 291-305
(in Japanese with English abstract).

Umehara, A. et al., 2015. Short-term dynamics of cyanobacterial toxins (microcystins) following a discharge from a coastal reservoir in Isahaya Bay, Japan. *Marine Pollution Bulletin,* 92(1-2), pp. 73-79.

Unoki, S. & Sasaki, K., 2007. On the system of abnormal changes of the environment induced by the big Isahayawan reclamation project in Ariake Bay. *Oceanography in Japan,* 16(4), pp. 319-328
(in Japanese).

Yamaguchi, S. & Hayami, Y., 2009. Behavior of low salinity water and its implication for the water quality after freshets at the head of the Ariake Sea. *Bulletin on Coastal Oceanography,* 46(2), pp. 161-173
(In Japanese with English abstract).

Yanagi, T. & Abe, R., 2003. Year-to-year variation of water exchange in Ariake Bay. *Oceanography in Japan,* 12(3), pp. 269-275 (In Japanese with English abstract).

Yanagi, T. & Abe, R., 2005. Increase in water exchange ratio due to a decrease in tidal amplitude in Ariake Bay, Japan. *Continental Shelf Research,* pp. 2174-2181.

Yanagi, T. & Shimomura, M., 2006. Seasonal variation in the transverse and layered structure of estuarine circulation in Ariake Bay, Japan. *Continental Shelf Research,* pp. 2598-2606.

Yano, S. & Nishimura, K., 2014. *Numerical analysis on the effect of large reclamation on the baroclinic structure in the Ariake Sea, Japan.* Hanoi, Vietnam, 6p., in USB memory

Yano, S. et al., 2010 (a). Analysis of Region of Freshwater Influence Based on Large-Scale In-Situ Observations in Ariake Sea. *Journal of Japan Society of Civil Engineers, Ser. B2 (Coastal Engineering),* 66(1), pp. 356-360 (In Japanese with English abstract).

Yano, S. et al., 2009. *Numerical Simulation of Nonlinear Barotropic Tide in Ariake Bay and Yatsushiro Bay, Japan.* Proc. of 3rd International Conference on Estuaries & Coasts, Sendai, Japan, pp. 159-166.

Yano, S., Winterwerp, J. C., Tai, A. & Saita, T., 2010 (b). Numerical Experiments on Features of Nonlinear Tide and Its Influences on Sediment Transport in the Ariake Sea and the Yatsushiro Sea. *Journal of Japan Society of Civil Engineers, Ser. B2 (Coastal Engineering),* 66(1), pp. 341-345 (in Japanese with English abstract).

Yuk, J.-H., Choi, B. H. & Kim, K. O., 2011. Changes of Tides in Isahaya Bay due to a Barrier. *KSCE Journal of Civil Engineering,* pp. 427-437.

Appendix

Comparisons of different scenarios

Scenario (2) – scenario (3): Temporal change of freshwater discharge for points b, c and d

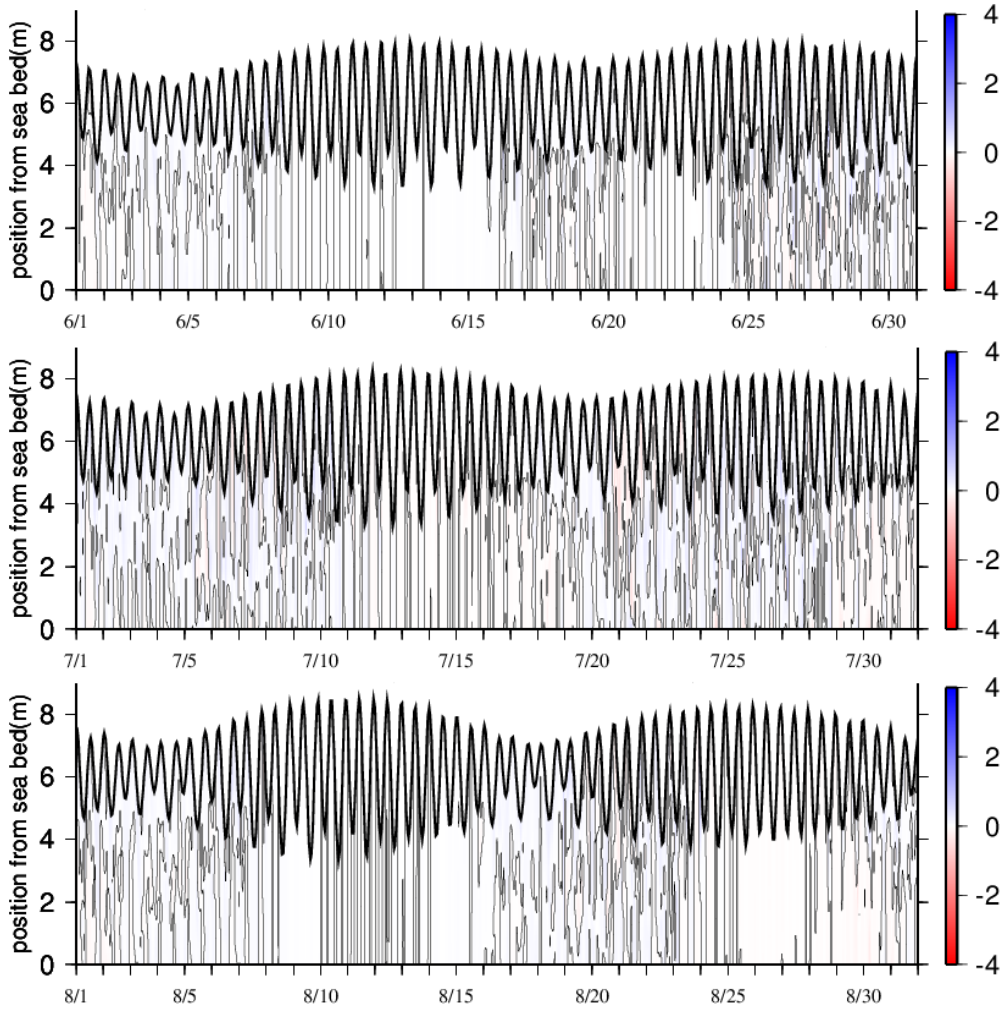

Figure 31 Amount of change in salinity at point b (scenario (2) – scenario (3))

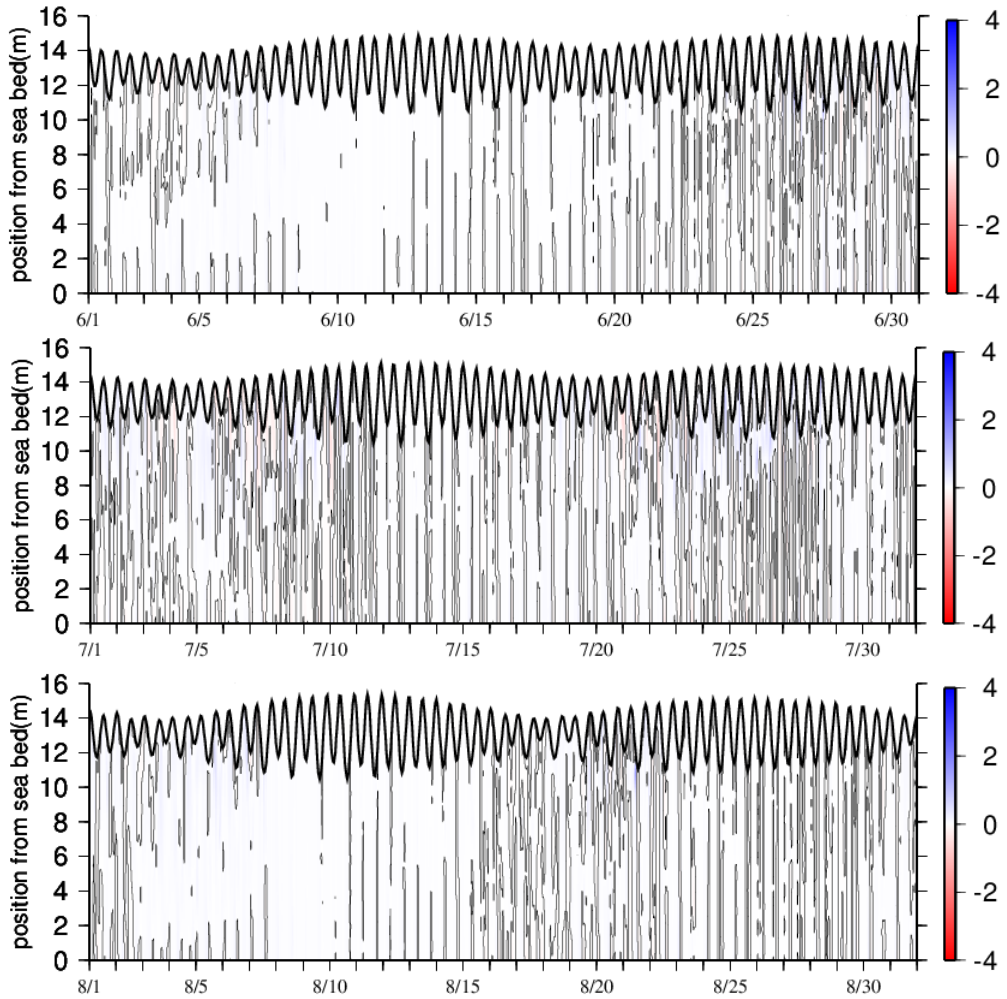

Figure 32 Amount of change in salinity at point c (scenario (2) – scenario (3))

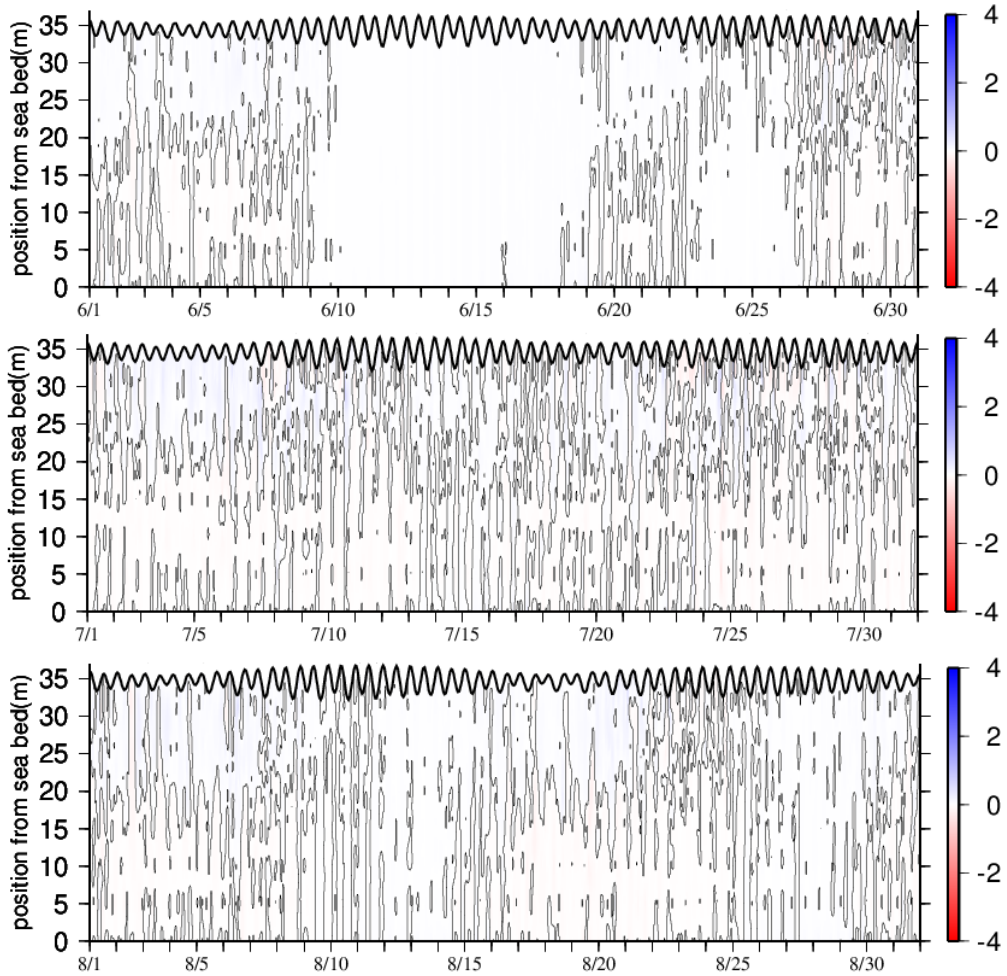

Figure 33 Amount of change in salinity at point d (scenario (2) – scenario (3))

Scenario (2) – scenario (1): Weakened vertical mixing, spatial and temporal change of freshwater discharge for points b, c and d

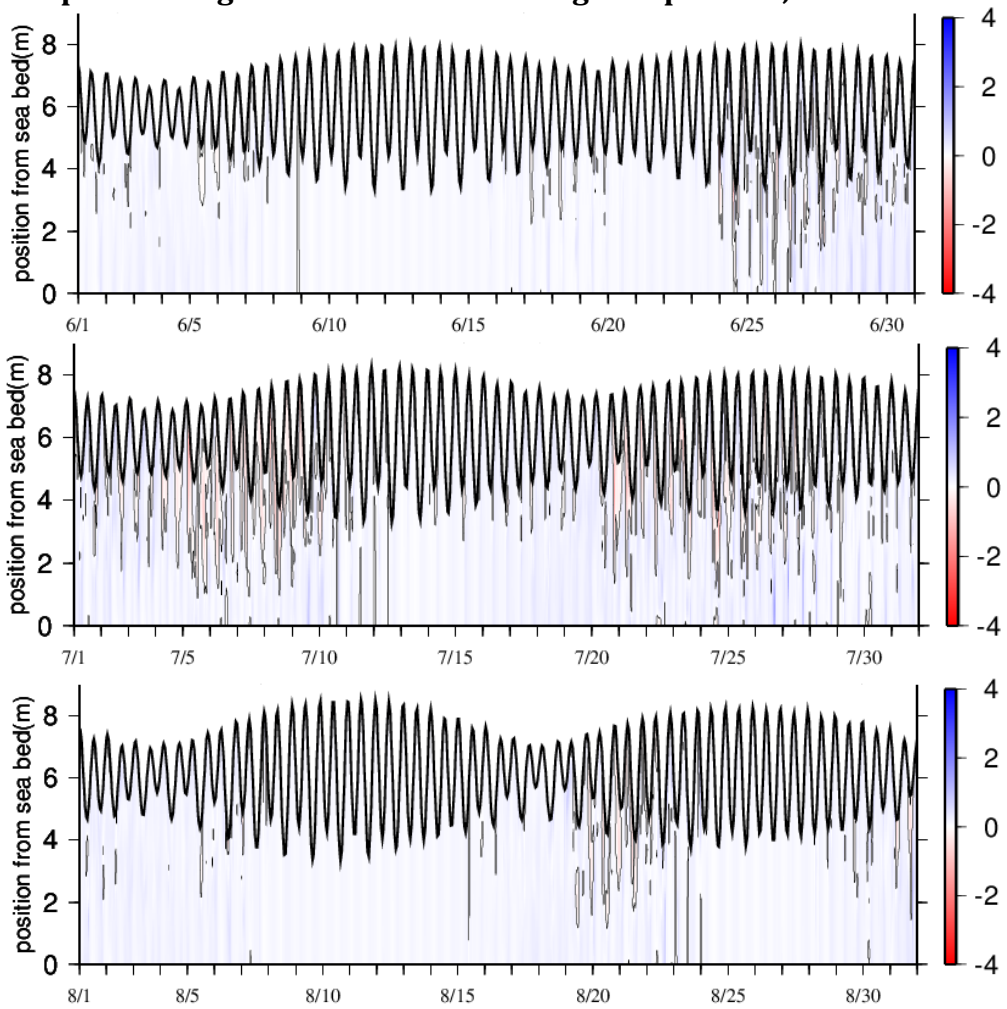

Figure 34 Amount of change in salinity at point b (scenario (2) - scenario (1))

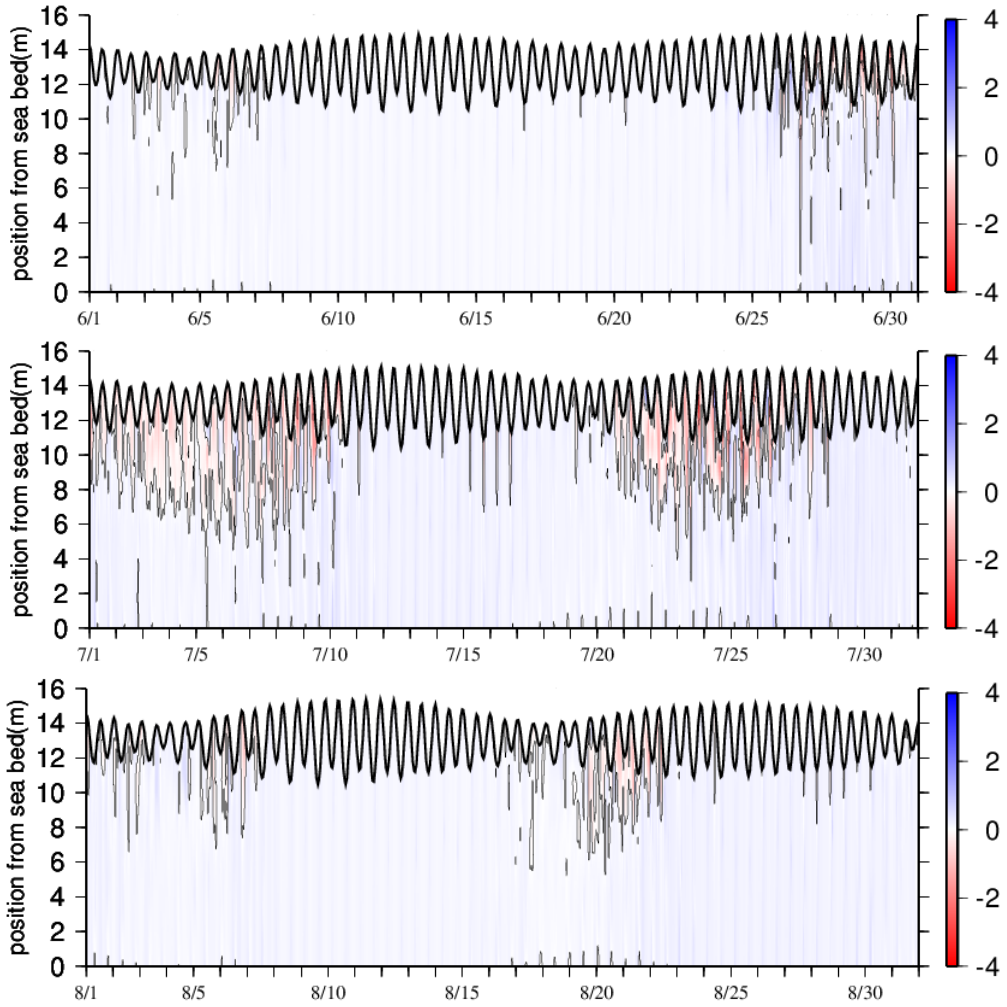

Figure 35 Amount of change in salinity at point c (scenario (2) - scenario (1))

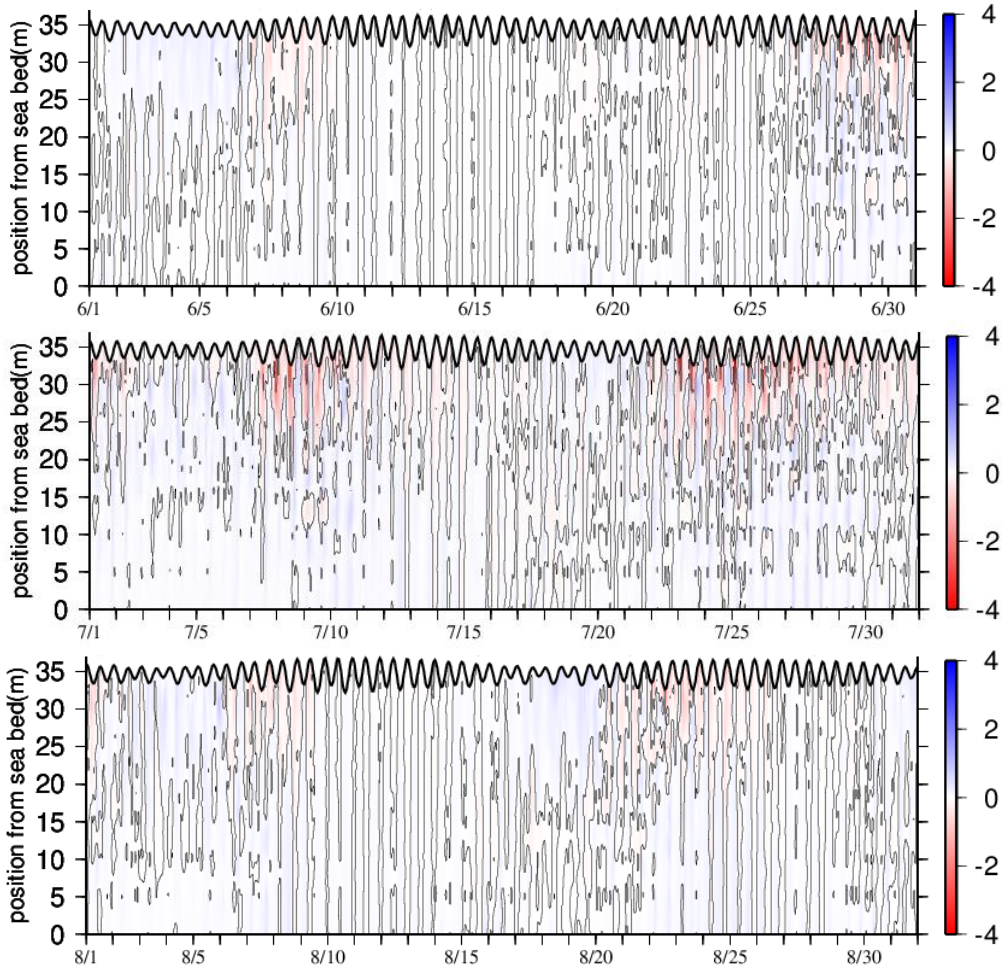

Figure 36 Amount of change in salinity at point d (scenario (2) - scenario (1))